

Interactive comment on

“Light-induced protein nitration and degradation with HONO emission”

by Hannah Meusel et al.

Anonymous Referee #1

General Comments:

This manuscript reports results of a study aimed at investigating photochemical formation of HONO from proteins exposed to NO₂. The study employs coated wall flow tube techniques with LOPAP detection of HONO and chemiluminescence detection of NO₂. The methods are appropriate for such a study and the results appear to meet the standards required by ACP. The topic is important as it addresses the byproducts associated with light-induced nitration of protein aerosols (e.g., pollen and other biological aerosols); it is novel in that it attempts to address the photochemical fate of the nitrated proteins.

The relevance of protein nitration to the potency of allergens has been discussed in several publications, so that is clear. However, it is not so clear that nitrated proteins will be an important component of the daytime HONO budget since proteinaceous aerosols would constitute only a minor fraction of the total aerosol surface area in the atmosphere. Furthermore, strong evidence has recently surfaced showing that the daytime HONO source is not linked to NO₂ (see Pusede et al. Environ. Sci. Technol. 2016). In addition, there are limited situations where the aerosol phase has proved to have an impact on atmospheric HONO concentrations. Perhaps the authors could add a more extensive discussion of settings where they predict this chemistry to be important? Regardless, it is my opinion that the chemistry presented is interesting enough to warrant publication after these issues are addressed.

Response:

Pusede et al., 2015 (Environ. Sci. Technol., 49, 12774-12781, 2015) observed no significant weekday-weekend difference in HONO levels during daytime, while NO₂ levels changed significantly during weekday-weekend and concluded that HONO didn't derive from NO₂. Several studies didn't find correlations with NO₂, but much more publications see a correlation with NO₂ and an enhanced correlation with NO₂*J (e.g. Costabile et al., 2010; Spataro et al., 2013; Sörgel et al., 2011 + 2015; Su et al., 2008; Lee et al., 2016), both being in line with our observations presented in here. The absence of NO₂-HONO correlation does not exclude the involvement of NO₂ conversion in HONO. Whatever the detailed mechanism is, there are many complex processes involved in aerosol particles and on the ground surface that could lead to a highly non-linear dependence on NO₂ in both concentration and time domains (HONO precursors may be stored in reservoirs, both in the physical and chemical senses). Besides heterogeneous photochemistry on aerosols also heterogeneous photoenhanced NO₂ conversion on ground surfaces has been proposed (Ren et al., 2011; Laufs et al., 2017). As proteins are found in both aerosol particles (coarse and fine mode) as well as on most ground surfaces (soil, leaf etc.), we think that their widespread occurrence provides reasonable justification to have a closer look into the characteristics of their HONO emissions. Indeed, we agree with the referee that pinning down their impact in individual settings is crucial, but for the time being, too uncertain to make a strong statement in here.

Comment:

Page 1, line 20: The authors write that “nitration degrees of about 1% were derived applying NO₂ concentrations...” How was the nitration degree determined?

Response:

The nitration degree is defined as the concentration of nitrated tyrosine divided by the concentration of all tyrosine residues. As it is written in the method part (2.1.), the nitration degrees were determined by HPLC-DAD analysis.

Nitrated tyrosine residues were detected at 357 nm (and 280 nm) while tyrosine residues were detected at 280 nm only.

The respective section in the method part of the manuscript (page 4 lines 13-15) was slightly modified:

“Absorbance was monitored at wavelengths of 280 (tyrosine) and 357 nm (nitrotyrosine). The sample injection volume was 10-30 µL. Each chromatographic run was repeated three times. The protein nitration degree, which is defined as the ratio of nitrated tyrosine to all tyrosine residues, was determined by the method of Selzle et al. (2013). Native and un-treated BSA did not show any degree of nitration. “

Comment:

1, 21: The term “Gas exchange measurements of TNM-nitrated proteins” is ambiguous.

Response:

Now corrected in the manuscript (page 1, lines 21-22) to: “Measurements of gas exchange on TNM-nitrated proteins...”

Comment:

1, 23: The term “fumigation” is not appropriate here. Please replace.

Response:

Now corrected to “NO₂ exposure...”

Comment:

3, 22-24: I note that nitrated ovalbumin (OVA) was used in only one experiment in this study (section 3.2.1) while bovine serum albumin (BSA) was used for everything else. Ideally, one would use one protein for all the studies to facilitate comparison of results. Please explain why one protein was not used for everything.

Response:

Unfortunately, only nitrated OVA but no nitrated BSA was available from our partner.

Comment:

3, 32: The methods section indicates that tetranitromethane is used to nitrate the OVA samples. This is a highly toxic and explosive reagent. Appropriate warnings should be included in this section to bring awareness of the dangers of using this reagent to anyone wishing to repeat these experiments.

Response:

Although in most other publications safety notes/warnings of toxic chemicals are not mentioned, we acknowledge the advice and now added a respective note in the manuscript (page 3, line 34-35):

“Please note that TNM is toxic if swallowed, can cause skin, eye and respiration irritation, is suspected to cause cancer and causes fire or explosion.”

Comment:

9, 33 (and other places in the text, e.g. 10, 14): The term “catalytic converter” is an engineering term and is not appropriate in this context. I would replace with “catalytic surface”.

Response:

Now corrected in the text according to the referee’s suggestion.

Comment:

10, 6: It is not clear what ND refers to in this line. Please clarify.

Response:

ND refers for nitration degree as in the whole manuscript. This abbreviation was introduced when first mentioned in the manuscript on page 5 lines 19/20 (original manuscript). The nitration degree is defined as the concentration of nitrated tyrosine divided by the concentration of all tyrosine residues (see also comment above).

Comment:

10, 27: *It seems to me the term $[HONO]1 + [HONO]2$ is incorrect. Instead of indicating concentrations, should one not be using rates (i.e., $d[HONO]1/dt + d[HONO]2/dt$)?*

Response:

Thank you very much for noting, indeed that's the case. Now corrected in the text as suggested by the referee and moved to a new supplement (see comment below).

Comment:

Kinetics studies section: The derivation of some of the indicated terms is not so clear. I question the need to go into the level of detail displayed in eq. 1-5. Please check over the derivation of k_{eff} . Also, perhaps I missed this explanation, but why are the reversible reactions in Figure 9 not included?

Response:

To simplify the calculations, the reversible processes of NO_2 were neglected (k_1 would be the effective rate constant for the adsorption; including adsorption and desorption). In addition, the adsorption of HONO to the protein surface is supposed to be very small in relation to the desorption, as proteins are slightly acidic (similar to k_1 k_3 would be the effective rate constant including desorption and adsorption).

Details are now displayed and discussed in a new supplement.

Comment:

Figure 1: Ozone is included above the arrow in the first step. However, there is no indication that ozone was used in this study. Please clarify or correct.

Response:

True, in our study only N_2 was applied as a carrier gas (no O_3). Fig. 1 is meant to give a complete overview of possible nitration mechanisms and refers to another study on nitration of proteins with O_3 and NO_2 (Shiraiwa et al., 2012 as indicated in the caption).

Figure 1 caption was modified: **“Overview on possible reaction mechanism...”**

Reference:

- Costabile, F., Amoroso, A., and Wang, F.: Sub-mu m particle size distributions in a suburban Mediterranean area. Aerosol populations and their possible relationship with HONO mixing ratios, *Atmospheric Environment*, 44, 5258-5268, 10.1016/j.atmosenv.2010.08.018, 2010.
- Laufs, S., Cazaunau, M., Stella, P., Kurtenbach, R., Cellier, P., Mellouki, A., Loubet, B., and Kleffmann, J.: Diurnal fluxes of HONO above a crop rotation, *Atmos. Chem. Phys.*, 17, 6907-6923, 10.5194/acp-17-6907-2017, 2017.
- Lee, J. D., Whalley, L. K., Heard, D. E., Stone, D., Dunmore, R. E., Hamilton, J. F., Young, D. E., Allan, J. D., Laufs, S., and Kleffmann, J.: Detailed budget analysis of HONO in central London reveals a missing daytime source, *Atmos. Chem. Phys.*, 16, 2747-2764, 10.5194/acp-16-2747-2016, 2016.
- Pusede, S. E., VandenBoer, T. C., Murphy, J. G., Markovic, M. Z., Young, C. J., Veres, P. R., Roberts, J. M., Washenfelder, R. A., Brown, S. S., Ren, X., Tsai, C., Stutz, J., Brune, W. H., Browne, E. C., Wooldridge, P. J., Graham, A. R., Weber, R., Goldstein, A. H., Dusanter, S., Griffith, S. M., Stevens, P. S., Lefer, B. L., and Cohen, R. C.: An Atmospheric Constraint on the NO_2 Dependence of Daytime Near-Surface Nitrous Acid (HONO), *Environmental Science & Technology*, 49, 12774-12781, 10.1021/acs.est.5b02511, 2015.

- Ren, X., Sanders, J. E., Rajendran, A., Weber, R. J., Goldstein, A. H., Pusede, S. E., Browne, E. C., Min, K. E., and Cohen, R. C.: A relaxed eddy accumulation system for measuring vertical fluxes of nitrous acid, *Atmospheric Measurement Techniques*, 4, 2093-2103, 10.5194/amt-4-2093-2011, 2011.
- Selzle, K., Ackaert, C., Kampf, C. J., Kunert, A. T., Duschl, A., Oostingh, G. J., and Poschl, U.: Determination of nitration degrees for the birch pollen allergen Bet v 1, *Analytical and Bioanalytical Chemistry*, 405, 8945-8949, 10.1007/s00216-013-7324-0, 2013.
- Shiraiwa, M., Selzle, K., Yang, H., Sosedova, Y., Ammann, M., and Poeschl, U.: Multiphase Chemical Kinetics of the Nitration of Aerosolized Protein by Ozone and Nitrogen Dioxide, *Environmental Science & Technology*, 46, 6672-6680, 10.1021/es300871b, 2012.
- Sörgel, M., Regelin, E., Bozem, H., Diesch, J. M., Drewnick, F., Fischer, H., Harder, H., Held, A., Hosaynali-Beygi, Z., Martinez, M., and Zetzsch, C.: Quantification of the unknown HONO daytime source and its relation to NO₂, *Atmospheric Chemistry and Physics*, 11, 10433-10447, 10.5194/acp-11-10433-2011, 2011.
- Sörgel, M., Trebs, I., Wu, D., and Held, A.: A comparison of measured HONO uptake and release with calculated source strengths in a heterogeneous forest environment, *Atmos. Chem. Phys.*, 15, 9237-9251, 10.5194/acp-15-9237-2015, 2015.
- Spataro, F., Ianniello, A., Esposito, G., Allegrini, I., Zhu, T., and Hu, M.: Occurrence of atmospheric nitrous acid in the urban area of Beijing (China), *The Science of the total environment*, 447, 210-224, 10.1016/j.scitotenv.2012.12.065, 2013.
- Su, H., Cheng, Y. F., Shao, M., Gao, D. F., Yu, Z. Y., Zeng, L. M., Slanina, J., Zhang, Y. H., and Wiedensohler, A.: Nitrous acid (HONO) and its daytime sources at a rural site during the 2004 PRIDE-PRD experiment in China, *Journal of Geophysical Research-Atmospheres*, 113, 10.1029/2007jd009060, 2008.

Anonymous Referee #2

Overview

In this paper, titled "Light-induced protein nitration and degradation with HONO emission" by Meusel et al., the authors present an interesting dataset focused on the uptake of NO₂ and subsequent emission of HONO by protein surfaces. HONO is an important reservoir for OH radicals and NO_x, but very little is known about its formation and subsequent photochemistry on the surface of aerosol particles, which represent a significant amount of reactive surface area in the atmosphere. Therefore, the topic is very much atmospherically relevant. Based on a series of flow tube experiments, the authors find a dependence of NO₂ uptake and subsequent emission of HONO on light intensity, relative humidity, NO₂ concentration, and flow tube coating thickness. The authors argue that surface-enhanced NO₂ conversion to HONO follows a Langmuir-Hinshelwood reaction mechanism. While I find the topic to be of general interest to the community, I have several concerns regarding the experimental approach and interpretation, and therefore request that the authors make significant revisions to their manuscript before publication in ACP after considering my comments listed below.

Comment:

Section 3.1 (lines 22-23): The authors indicate that additional continuous exposure of the protein surface by light fully decomposed the protein so that no intact protein could be detected. However, the authors should clarify if only the nitrated protein residues decompose or all (nitrated and non-nitrated), and how that might affect ND.

Response:

The nitration degree in this study was detected with HPLC-DAD which only can detect the intact protein and the nitrated protein, but no possible degradation products like peptides, single amino acids and their nitrated forms, as those compounds are "filtered out" by the chromatography. According to our HPLC-DAD results also the non-nitrated proteins decomposed, i.e., the peak was below detection limit. If only nitrated-proteins decompose, the results would indicate that all proteins were firstly nitrated prior of being decomposed. Amino acids and peptides might still be present, either nitrated or not.

Now better specified in the main text of the manuscript (page 5, line 27): “Note that no intact protein (nitrated and non-nitrated) could be detected by HPLC-DAD after another 20 hours of irradiation without NO₂, indicating light induced decomposition of proteins”

Comment:

Could the authors discuss the atmospheric implications of the irradiance intensity applied in this study compared to the solar irradiance intensity? They mention that their irradiance was 40% of clear sky conditions, similar to cloudy days, so does that imply that this chemistry could be more relevant in the atmosphere than the results suggest? Please elaborate.

Response:

There are two different processes to discuss: 1) the degradation of nitrated proteins with HONO formation and 2) the heterogeneous NO₂ conversion. As shown in Fig.3 the light dependency of HONO formation from previously nitrated proteins is almost linear in the range of applied light intensity. So here, yes during sunny days, when irradiance is higher than our applied light intensity, an even higher HONO formation can be anticipated, accompanied by a faster degradation of the nitrated proteins. However, as the dependency for higher light intensities was not investigated, we cannot make a firm statement here. The observed light dependency of the heterogeneous conversion of NO₂ on BSA was not linear as shown in Fig. 4b. Here our results rather indicate an upper limit for the HONO formation, as was reported similarly by Stemmler et al. (2006, 2007).

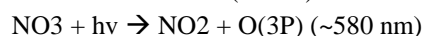
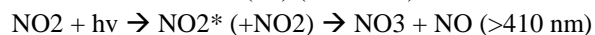
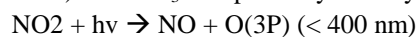
Now added in the conclusion (page 13, line 4-7): “While heterogeneous HONO formation of BSA exposed to NO₂ revealed light saturation at intensities higher than 161 W m⁻², the HONO formation from previously nitrated OVA was linearly increasing over the whole light intensity range investigated. The latter let assume even higher HONO formation under sunny (clear sky) ambient atmospheric conditions.”

Comment:

In the VIS light wavelength range of the lamps used in this study (between 400 nm and 700 nm), NO₂ photolysis could be significant and play an important role in the degree of protein nitration and HONO production. Was NO₂ photolysis a concern and how might it affect the results?

Response:

Direct NO₂ photolysis (<400 nm) won't occur under conditions applied in this study (Gardner et al., 1987; Roehl et al., 1994). There might be some electronic excitation of NO₂, which disproportionate to NO and NO₃. Stemmler et al., 2007, determined a photolysis frequency of NO₂ of up to 5 x 10⁻⁴ s⁻¹ for very similar light conditions as we used, which is much lower than in the atmosphere (e.g. up to 1 x 10⁻² during the CYPHEX campaign 2014, Meusel et al., 2016). But NO₃ will probably directly deplete under this irradiation back to NO₂ or NO (Johnston et al., 1996).



Overall we assume the effect to be negligible. Furthermore, Shiraiwa et al. (2012) could exclude the importance of NO₃ (in their case formed by reaction of NO₂ + O₃) uptake on BSA.

Now added in section 3.1 (page 6, lines 16-23): “Shiraiwa et al. (2012) performed kinetic modelling and found that maximum 30% (conservative upper limit) of N-uptake on BSA could be explained by NO₃ or N₂O₅, which are generated by the reaction of NO₂ and O₃, while overall nitration was governed by an indirect mechanism in which a radical intermediate was formed by the reaction of BSA with ozone, which then reacted with NO₂. On NaCl surface N-uptake was dominated by NO₃ and N₂O₅. Furthermore, NO₃ radicals, which in this study could be formed by photolysis of NO₂ (>410 nm, disproportionation of excited NO₂), are not stable under the light condition applied (400-700 nm) (Johnston et al., 1996). Therefore, in the present study reactions with NO₃ were neglected. Photolysis of NO₂ forming NO (< 400 nm) can also be neglected (Gardner et al., 1987; Roehl et al., 1994). A photolysis

frequency for NO₂ of up to 5 x 10⁻⁴ s⁻¹ under similar experimental light conditions was determined by Stemmler et al., 2007.”

Comment:

In the last paragraph of the results section 3.1, the authors compare their results, which were conducted in the presence of NO₂, with other nitration studies conducted in the presence of both NO₂ and O₃. How are these comparable, since NO₂ and O₃ combine to make N₂O₅ and NO₃, which is a much more effective nitrating agent? The authors argue that their low ND may be due to light exposure, whereas the studies with larger ND that they compare to were conducted in the dark in the presence of NO₃, so wouldn't the authors expect more ND in the other studies anyway because of the higher reactivity of NO₃?

Response:

Shiraiwa et al. (2012) estimated that maximum 30% of the N-uptake is due to NO₃ and N₂O₅ uptake on BSA, while overall nitration was governed by an indirect mechanism in which a radical intermediate was formed by the reaction of BSA with ozone, which then reacted with NO₂. On NaCl surfaces, on the other hand, NO₃ and N₂O₅ uptake dominate. Therefore, the higher ND of BSA exposed to O₃ and NO₂ is mainly due to higher activation by O₃ and due to BSA decomposition by light. Please also see the comment above.

Comment:

Section 3.2.4: The authors conclude that HONO production is greater for larger protein coating thicknesses. However, the coatings also covered different surface area of the flow tube. Do you expect surface area to be important in the context of this study? My concern is that by shortening the coated length of the flow tube for the thicker coating experiments, the authors potentially introduce bias in their measurement since both NO₂ and HONO are exposed to different coated surface areas of the flow tube. Following NO₂ uptake by the shorter coated length flow tube, the HONO that is emitted is subsequently exposed to less coated surface area for the remaining length of the flow tube. If a fraction of the HONO is taken up by the protein surface, less protein surface area implies more of the HONO is present in the gas phase. A better approach would have been to either maintain the same length of coated flow tube between experiments or to maintain the same surface concentration of protein between experiments for different coated lengths. The authors should at least discuss potential caveats for changing the coated surface area of the flow tube between experiments.

Response:

As we manually coated the reaction tube, it was difficult to obtain equally/consistent surfaces. Therefore, each coating was different and also the covered surface area could only be roughly estimated. So, we agree with the referee that the coating thickness/surface is the biggest uncertainty in the experiment. And yes, there might be a bias based on NO₂/HONO uptake/emission on/from different coating surface areas. But we expect that HONO uptake coefficients on both proteins (as slightly acidic) as well as on glass surfaces were small (Syomin and Finlayson-Pitts, 2003), so that the difference of HONO uptake due to different surface areas and covered tube length is low. Also NO₂ uptake on glass is supposed to be significantly lower than on proteins. We don't expect a difference in tube coverage of 20% would increase HONO concentrations about three times.

According to the referee's suggestion, we now added in the main text (page 8, lines 19-24): “Exposing (20%) different coated surface areas in the flow tube, potentially introduced bias comparing different data sets. Emitted HONO might be re-adsorbed differently by proteins and glass surface. However, as the protein is slightly acidic, a low uptake efficiency of HONO by BSA can be anticipated, which should not differ too much from the un-covered glass tube surface (Syomin and Finlayson-Pitts, 2003). Accordingly, NO₂ uptake on glass is assumed to be significantly lower than on proteins.”

Comment:

The rate of HONO emission decay as a function of exposure time as presented in Fig. 6 is also a bit confusing; the authors report emission decay rates in the range of 10-20 ppt hr⁻¹, but it is difficult to tell from the y-axis since [HONO] is reported in ppb. It would help if the y-axis and reported rates had the same concentration units. The authors might also consider changing their y-axis to a log scale or plotting the red data points on a separate y axis, so the reader can better observe the decay for different time periods. However, it appears the rate is more on the order of 160 ppt hr⁻¹ (linearly interpolated between 0 and 3 hrs). Why were the HONO emission decay rates only reported near the end of the exposure period (assuming the reported rates cover the exposure periods indicated by the arrows in Fig. 6)?

Response:

Fig. 6 does not show emission rates as a function of time, but normalized (to reaction tube coverage) HONO concentrations vs time! The numbers in the diagram represent the slope (decay rates) at the end (time period indicated by arrows), and indicate a stable HONO formation (as also seen in Fig.8). In figure 8 also several decay rates are shown for earlier exposure times, so that in the respective figure 6 the decay rates are only shown in the end when the concentrations are stable.

The unit of the y axis was changed from ppb to ppt.

Comment:

Given the apparent strong dependence on coating thickness, how relevant are the thicknesses of the coatings applied to the flow tube (>200 nm) compared to typical atmospheric aerosol? The authors should at least discuss the implications of coating thickness and HONO formation in the context of atmospheric aerosol particles.

Response:

Typical aerosol concentrations of bacteria, fungal spores and pollen are 0.1, 0.1-1 and 1 μg m⁻³, respectively (Despres et al., 2012). Aerosol particles may contain up to 5% proteins. But it is not known how much proteins cover the aerosol surface nor how thick this coating would be. This was already mentioned in the conclusion part of the manuscript; and which is why it is hard to make a firm statement here. However, to address this important issue we now added in the text (page 13, lines10-17): “Typical aerosol surface concentrations in rural regions are about 100 μm² cm⁻³. Stemmler et al. (2007) estimated a HONO formation of 1.2 ppt h⁻¹ on pure humic acid aerosols in environmental conditions. As NO₂ uptake coefficients and HONO formation rates on proteins are similar to humic acid but only about 5% of the aerosol mass can be assumed to consist of proteins, it can be anticipated that HONO formation on aerosol is not a significant HONO source in ambient environmental settings. However, proteins on ground surfaces (soil, plants etc.) might play a more important role. Accordingly, Stemmler et al. (2006 and 2007) suggested that NO₂ conversion on soil covered with humic acid would be sufficient to explain missing HONO sources up to 700 ppt h⁻¹.”

Comment:

Section 3.2.6: Have the authors considered to what extent photolysis of HONO (in the case of the UV/VIS experiment) plays in the temporal evolution of the HONO concentration? The authors argue that the plateau in the HONO concentration in Fig. 8, followed by continuous and relatively stable emission of HONO from the protein surface is consistent with a Langmuir-Hinshelwood reaction mechanism. However, HONO photolyzes under UV conditions (300 nm < λ < 400 nm), so might there be a point when the temporal HONO emission profile becomes limited by photolysis? The authors might consider including a photolysis term in their kinetics calculation (for both NO₂ and HONO), e.g. $d[NO_2]_g/dt = k_1[NO_2]_g - j(NO_2)[NO_2]_g$ and $d[HONO]_g/dt = k_3[HONO]_g - j(HONO)[HONO]_g$.

Response:

HONO photolysis was not considered. The overlap of UV light spectrum and HONO absorption/photolysis spectrum is quite low about 340-400 nm. The quartz glass tube has a transmission of 90% at these wavelengths. The applied light intensity (with 7 lights on) is about 40% of a clear sky irradiance for a solar zenith of 48°. In clear sky HONO

photolysis frequencies are in the range of $1.2\text{-}1.5 \times 10^{-3} \text{ s}^{-1}$ (e.g., on Cyprus in summer 2014; Meusel et al. 2016). In the reaction tube the photolysis frequency would therefore decrease down to $0.4\text{-}0.5 \times 10^{-3} \text{ s}^{-1}$. When only irradiated with VIS lights (exclusion of HONO photolysis, emission profile not limited) the pattern is the same as with UV (only a smaller absolute concentration) indicating a stable formation.

Now revised in the manuscript in the kinetic section (page 11, line 34 – page 12 line 3): “In this study, neither HONO nor NO₂ photolysis is considered, as the overlap of the applied UV/VIS or VIS range (340-700 nm or 400-700 nm) and the HONO and NO₂ photolysis spectrum (<400 nm) is low. Furthermore, the applied light intensity is lower compared to clear sky irradiance and the respective UV light is partly absorbed by the reaction tube although quartz glass was used (transmission ~ 90%) and the photolysis frequency would decrease down to 10^{-4} s^{-1} . Hence, the photolysis is assumed to be not significant.”

Comment:

Section 3.3 and Fig. 8: a) Here, it appears the authors apply a series of kinetic equations to describe the temporal HONO emission profile shown in Fig. 8 based on Langmuir-Hinshelwood reaction kinetics. First, it is unclear if the lines plotted on top of the “UV/VIS” blue line in Fig. 8 are actually based on the kinetic equations described in section 3.3 or if they are simply linear fits with no theoretical basis, because in the figure description it states, “Straight lines: : :show the regressions: : :” If they are simply linear fits and then the kinetic terms were derived from the linear regression, my concern is this introduces significant ambiguity in the derived kinetics terms, because then the choice for each modeled section is entirely dependent on the user and not based on a sound theoretical description. Please clarify in both the Fig. 8 description and in sec. 3.3 whether these are simply linear fits or modeled based on the kinetic equations described in sec. 3.3. Furthermore, the authors must clarify what values were used (or derived from the linear fit) for k_1 , k_2 , k_3 , k_4 , k_5 , and k' .

b) As a sensitivity test and validation of their model, I encourage the authors to apply their derived kinetic terms to model [HONO] as a function of [NO₂], as shown in Fig. 5. Can [HONO] as a function of [NO₂] be reproduced from the Langmuir-Hinshelwood terms described in sec. 3.3? Regarding Fig. 5, what do the dashed lines represent, are they fits to the data or just there to guide the eye? Please clarify in the figure description.

c) Alternatively, the authors could plot their derived uptake coefficients (instead of [HONO]) as a function of time, and apply the Langmuir-Hinshelwood framework, e.g., as described in Ammann et al. [2003]. This would also enable derivation of key kinetic terms describing NO₂ uptake by proteinaceous aerosol surfaces, including the Langmuir equilibrium constant, surface accommodation coefficient and second-order surface reaction rate constant, which the community might find useful.

Response:

a) The lines in fig 8 are linear fits (no theoretical basis). The slopes of those were taken to calculate k_{eff} .

Other rate constants (k_1 , k_2 , k_3 , k_4 , k_5 , k') were not calculated. Single equations were moved to a new supplement.

b) In fig 5. the dotted lines are regressions of the measured data points (exponential fittings, e.g., $y = y_0 + A * e^{-x/t}$) only to guide the eye (now better described in the figure captions).

In our kinetic study we calculated an effective rate constant for the NO₂ conversion on BSA. In a range of 0-100 ppb NO₂ the HONO formation is almost linear (fig 5), which would be also indicated by the Langmuir-Hinshelwood mechanism (here first rate: $d[\text{HONO}]/dt = k * [\text{NO}_2]$).

c) It is not possible to extract a full set of parameters for a LH model based on the present data. As pointed out in Bartels-Rausch et al. (2010) and to some degree also in the Stemmler et al. studies, the saturating behavior of photochemical HONO production may be due to either the adsorbed precursor on the surface or due to a photochemical competition process, which also leads to a Lindemann-Hinshelwood type kinetic expression (Minero, 1999). Therefore, mathematically, the rate expressions get a comparable NO₂ pressure dependence. Therefore, measurements of the NO₂ dependence at different light intensities would be required to disentangle the two. The nearly single exponential (linear in the log-log plot) decay of gamma vs time in the figure below (fig. R1) indicates that the system is governed by degradation and not by reaction steady state, so that modelling the system explicitly in terms of all the kinetic parameters would be ambiguous.

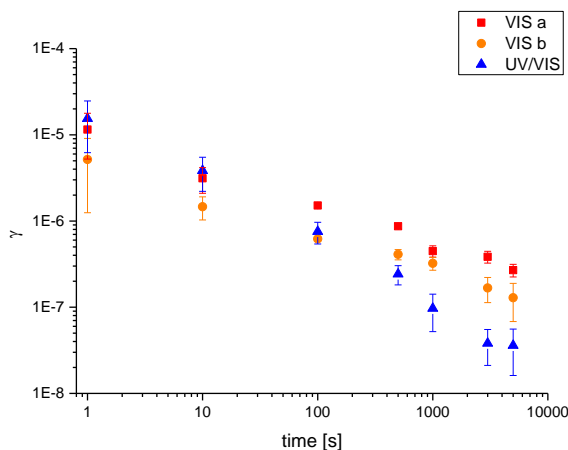


Fig. R1: log-log plot of the uptake-coefficients vs time for the three different experiments, indicated with the different colors (from the long term and kinetic study)

Added to the manuscript (page 12, lines 24-28): “It was not possible to extract a set of parameters for a Langmuir Hinshelwood mechanism (like Langmuir equilibrium constant, surface accommodation coefficient or second order rate constant) from the presented data. The saturating behavior of photochemical HONO production may be due to either the adsorbed precursor on the surface or due to a photochemical competition process, which also leads to a Lindemann-Hinshelwood type kinetic expression (Minero, 1999).”

Comment:

Have the authors considered the impact of photolysis of adsorbed HNO₃ on the production of HONO in this study? HNO₃(ads) + h_ν → HONO + O

Given the high relative humidity and [NO₂], HNO₃ adsorption or formation on the surface of the flow tube could be substantial. While there was some mention in the introduction that HONO production from the photolysis of HNO₃ may be important on organic substrates and soot, it was not discussed in the context of this study. The authors might consider estimating the contribution of adsorbed HNO₃ photolysis to HONO produced in their flow tube experiments. Adsorbed HNO₃ could be estimated based on the applied relative humidity and [NO₂] (and assuming some reasonable surface coverage of HNO₃), and the photolysis rate of HNO₃, e.g., as determined in a very recent study by Laufs and Kleffmann [2016].

Response:

Gas phase reaction doesn't produce HNO₃, because N₂, but not synthetic air was used as the carrier gas. Usually HNO₃ photolysis happens at < 350 nm. Photolysis of adsorbed HNO₃ might be shifted to slightly higher wavelength. In the publication of Laufs and Kleffmann (2016), J values (HNO₃→HONO) as low as 10⁻⁷ s⁻¹ were obtained. Our UV lamps had a spectral range of 340-400 nm. As a conclusion, HNO₃ photolysis was negligible in this study. Added to the section 3.2.6 (page 10, lines 18-23), as only here UV light was applied: “HONO formation by photolysis of (adsorbed) HNO₃ is assumed to be insignificant in this study. With N₂ as carrier gas, gas phase reactions of NO₂ do not produce HNO₃. Even when small amounts of HNO₃ would be formed by unknown heterogeneous reactions, photolysis of HNO₃ is only significant at wavelengths < 350 nm, which is close to the lowest limit of the UV wavelength applied in this study. Likewise, the respective photolysis frequency recently proposed by Laufs and Kleffmann (2016) of about 2.4 x 10⁻⁷ s⁻¹ is very low. ”

Minor Comment:

Page 6, lines 8-9: It's not clear what the authors mean by “condensing condition” at a relative humidity (RH) of 98%, but not at 92%? Does this mean that the protein undergoes deliquescence at RH=98% and not 92%?

Response:

At 98% RH water vapor condensed (visible water layer), but not at lower RH of 92% (Reinmuth-Selzle et al., 2013). Deliquescence of BSA already occurs at 35% (see section 3.2.4).

Minor Comment:

Figure 6: Along with the surface concentration of the coating (in units of $\mu\text{g cm}^{-2}$), please include the calculated thickness of the coating in units of nm.

Response:

According to the referee's advice, we now added the layer thickness in the plot:

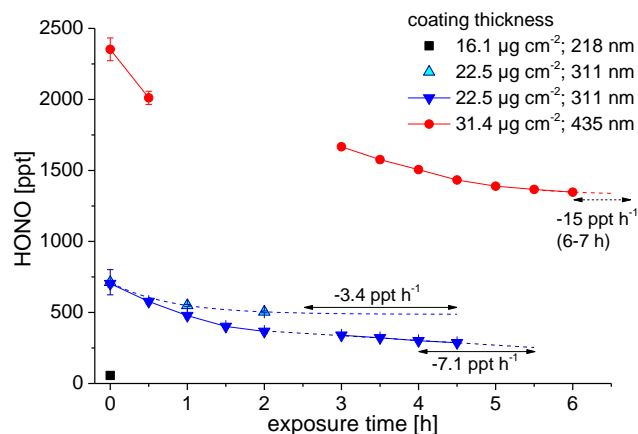


Fig. R2 = new Fig. 6: HONO concentration vs exposure time for different coating thicknesses.

Minor Comment:

Summary and conclusions section, page 11 line 34: What is the significance of 1m² of BSA surface or how was that surface area chosen?

Response:

HONO formation per m² [ppt h⁻¹ m⁻²]

Now the main text of the manuscript (page 13, lines 2-4) is rephrased to: “At 20 ppb NO₂ HONO formation of 19.8 ppb h⁻¹ m⁻² could be estimated”

References

- Ammann, M., U. Poschl, and Y. Rudich: Effects of reversible adsorption and Langmuir-Hinshelwood surface reactions on gas uptake by atmospheric particles, *Phys Chem Chem Phys*, 5(2), 351-356, 2003.
- Bartels-Rausch, T., Brigante, M., Elshorbany, Y. F., Ammann, M., D'Anna, B., George, C., Stemmler, K., Ndour, M., and Kleffmann, J.: Humic acid in ice: Photo-enhanced conversion of nitrogen dioxide into nitrous acid, *Atmos. Environ.*, 44, 5443-5450, 2010.
- Laufs, S., and J. Kleffmann: Investigations on HONO formation from photolysis of adsorbed HNO₃ on quartz glass surfaces, *Phys. Chem. Chem. Phys.*, 18, 9616-9625, 2016.
- Després, V., Huffman, J. A., Burrows, S. M., Hoose, C., Safatov, A., Buryak, G., Fröhlich-Nowoisky, J., Elbert, W., Andreae, M., Pöschl, U., and Jaenicke, R.: Primary biological aerosol particles in the atmosphere: a review, *Tellus B: Chemical and Physical Meteorology*, 64, 15598, 10.3402/tellusb.v64i0.15598, 2012.
- Gardner, E. P., Sperry, P. D., and Calvert, J. G.: Primary quantum yields of NO₂ photodissociation, *Journal of Geophysical Research: Atmospheres*, 92, 6642-6652, 10.1029/JD092iD06p06642, 1987.
- Johnston, H. S., Davis, H. F., and Lee, Y. T.: NO₃ Photolysis Product Channels: Quantum Yields from Observed Energy Thresholds, *The Journal of Physical Chemistry*, 100, 4713-4723, 10.1021/jp952692x, 1996.

- Meusel, H., Kuhn, U., Reiffs, A., Mallik, C., Harder, H., Martinez, M., Schuladen, J., Bohn, B., Parchatka, U., Crowley, J. N., Fischer, H., Tomsche, L., Novelli, A., Hoffmann, T., Janssen, R. H. H., Hartogensis, O., Pikridas, M., Vrekoussis, M., Bourtsoukidis, E., Weber, B., Lelieveld, J., Williams, J., Pöschl, U., Cheng, Y., and Su, H.: Daytime formation of nitrous acid at a coastal remote site in Cyprus indicating a common ground source of atmospheric HONO and NO, *Atmos. Chem. Phys.*, 16, 14475-14493, 10.5194/acp-16-14475-2016, 2016.
- Minero, C.: Kinetic analysis of photoinduced reactions at the water semiconductor interface, *Catal. Today*, 54, 205-216, 1999.
- Reinmuth-Selzle, K., Ackaert, C., Kampf, C. J., Samonig, M., Shiraiwa, M., Kofler, S., Yang, H., Gadermaier, G., Brandstetter, H., Huber, C. G., Duschl, A., Oostingh, G. J., and Pöschl, U.: Nitration of the Birch Pollen Allergen Bet v 1.0101: Efficiency and Site-Selectivity of Liquid and Gaseous Nitrating Agents, *Journal of Proteome Research*, 13, 1570-1577, 10.1021/pr401078h, 2014.
- Roehl, C. M., Orlando, J. J., Tyndall, G. S., Shetter, R. E., Vazquez, G. J., Cantrell, C. A., and Calvert, J. G.: Temperature Dependence of the Quantum Yields for the Photolysis of NO₂ Near the Dissociation Limit, *The Journal of Physical Chemistry*, 98, 7837-7843, 10.1021/j100083a015, 1994.
- Shiraiwa, M., Selzle, K., Yang, H., Sosedova, Y., Ammann, M., and Poeschl, U.: Multiphase Chemical Kinetics of the Nitration of Aerosolized Protein by Ozone and Nitrogen Dioxide, *Environmental Science & Technology*, 46, 6672-6680, 10.1021/es300871b, 2012.
- Syomin, D. A. and Finlayson-Pitts, B. J.: HONO decomposition on borosilicate glass surfaces: implications for environmental chamber studies and field experiments, *Physical Chemistry Chemical Physics*, 5, 5236-5242, 2003.
- Stemmler, K., Ammann, M., Donders, C., Kleffmann, J., and George, C.: Photosensitized reduction of nitrogen dioxide on humic acid as a source of nitrous acid, *Nature*, 440, 195-198, 10.1038/nature04603, 2006.
- Stemmler, K., Ndour, M., Elshorbany, Y., Kleffmann, J., D'Anna, B., George, C., Bohn, B., and Ammann, M.: Light induced conversion of nitrogen dioxide into nitrous acid on submicron humic acid aerosol, *Atmospheric Chemistry and Physics*, 7, 4237-4248, 2007.

Anonymous Referee #3

This MS reports on HONO formation resulting (mostly) from the interaction of NO₂ with a particular protein under visible illumination in a flow tube reactor. The HONO released to the gas phase is formed both by photolysis of nitrated tyrosine and a Langmuir-Hinshelwood surface reaction involving NO₂ uptake; this latter process forms HONO even in the dark. For both dark and illuminated channels, there is a positive dependence on RH which suggests that water is involved somehow, although this may be by changing the protein surface morphology rather than as a chemical promoter. The experiments are well constructed and the results are of some interest. I do have a few comments for the authors' consideration, however:

Comment:

page 5, lines 28-29: I am not convinced that you have demonstrated nitration with the very small signal reported.

Response:

The nitration degree was determined by HPLC-DAD as described elsewhere (Selzle et al., 2013). This technique is sensitive and well established (detection limit < 1%). The difference of the nitration degree of native BSA (ND = 0%) and BSA treated with NO₂/light (ND = 1%) is significant. Yes, it is a small nitration degree, but still nitration was detected!

Now modified in the main text (page 5 lines 25-26): "...nitration degree...by means of HPLC-DAD was (1.0±0.1)%., significantly higher than the ND of untreated BSA (0%)"

Comment:

page 6, lines 3-5: *Again, this is one possible inference, but is certainly not conclusively shown!*

Response:

We tune down the tone and it now reads, "...possibly suggesting the deficiency..."

Comment:

page 6, section 3.2.1: *this experiment is very poorly described - please explain exactly what was done.*

Response:

The method part (2.1 and 2.2) describes the procedure of the experiments and gives an overview on conditions... (table 1). In this experiment previously nitrated OVA (method part) was coated on a tube and irradiated with light (0,1,3,7 lights) while flushing with either zero air or 20 ppb NO₂. HONO emissions were detected at the outlet. After the trace gas exchange measurements the protein was extracted by pure H₂O and nitration degree was determined via HPLC-DAD.

Now modified in the main text: "To study HONO emission from nitrated proteins, OVA was nitrated with TNM (see section 2.1) in liquid phase. The nitrated OVA (2 mg; ND = 12.5%) was coated onto the reaction tube and exposed to VIS lights under either pure nitrogen flow or 20 ppb NO₂ gas. Strong HONO emissions were found..."

Comment:

Page 6, line 32-33: *Could this be related to the photodecomposition of the protein, reposted above?*

Response:

Yes indeed, as it was already stated in the main text: "...which is in line with the observed decomposition of the native protein presented above."

Comment:

Sections 3.2.2 and 3.2.3: *Brigante et al (J. Phys. Chem. A 2008, 112, 9503–9508) made these same observations.*

Response:

Brigante et al., (2008) observed a linear dependency of NO₂ loss (ln c₀/c) to light intensity (number of photons) for the NO₂ uptake on pyrene. Furthermore, they plotted NO₂ uptake coefficient as function of NO₂ concentration and shows an exponential (decay) dependence. They found that roughly 15% of the NO₂ loss on pyrene accounts for HONO production. Both cannot be directly compared to our results ("saturation" of HONO formation at high light intensities and very high NO₂ concentration).

However, Brigante is now additionally cited when discussing similarities to other studies.

Comment:

Page 8, line 19-20: *On what basis do you claim that nitration / reaction takes place below the surface layer?*

Response:

Indeed, the dependency of layer thickness on the HONO formation is a complex matter. Light penetrates into the bulk (according to the set-up illumination is from outside - light will first pass the protein layer at the inner glass surface and then the layer in contact with the carrier gas) and hence activation of the aromatic residues of the protein and photolysis of nitrated proteins can occur in the bulk. Also NO₂ might diffuse into the bulk (depending on humidity and therefore viscosity/solid or semi-solid state), and the formed HONO would also be able to diffuse out of the bulk. But we didn't mean to say that the reaction takes place only below the surface. Our point is that the observed dependence on the coating thickness suggests the Indeed, the dependency of layer thickness on the HONO formation is a complex matter. Light penetrates into the bulk (according to the set-up illumination is from outside - light will first pass the protein layer at the inner glass surface and then the layer in contact with the carrier gas) and

hence activation of the aromatic residues of the protein involvement of bulk reactions and the reactions can happen in both, surface and bulk phase.

We added one more conclusively sentence to the manuscript: “The observed dependence on the coating thickness suggests the involvement of the bulk reactions, but the reactions can happen in both, surface and bulk phase.”

Comment:

page 8, line 28, ff: Brigante et al (2008) also saw no RH dependence for NO₂/HONO on solid pyrene.

Response:

Now additionally cited in the manuscript: “No impact of humidity on NO₂ uptake coefficients on pyrene was detected (Brigante et al., 2008)”

Comment:

page 10, Eq. 1 and kinetic arguments: Why is the desorption reaction not included here? The implication of the L-H mechanism, suggested in Fig 5, is that this should be important. The kinetic scheme should reflect this, I think.

Response:

To simplify the calculations, the reversible processes were neglected. In addition, the adsorption of HONO to the protein surface is supposed to be very small in relation to the desorption as proteins are slightly acidic (please see respective comments/reply of referee #1)

Modifications in the manuscript accordingly to referee #1: the equations of the single processes (eq.1-5) were removed to a new supplement and only the final equation is shown.

Comment:

page 11, lines 17-23: This paragraph seems out of place here; perhaps in the Conclusions? In its place - can the authors in any way (semi)quantify their suggestion that HONO production via NO₂/protein interactions could be atmospherically important?

Response:

Paragraph moved to section 3.2.1 (page 7, lines 3-9)

See also referee 2 conclusion section (page 13, lines 10-17)

Comment:

The figure captions are not very descriptive. They should be rewritten, to explain what is displayed in the figures.

Response:

The figure captions were modified:

The term “normalized HONO” (several y-axes) was changed to “scaled HONO”.

Fig. 1: Overview on possible reaction mechanisms of atmospheric BSA nitration and subsequent HONO emission. The tyrosine phenoxyl radical intermediate is either formed by the reaction of tyrosine with a) NO₂, b) light or c) ozone. A second reaction with NO₂ forms 3-nitrotyrosine (was adapted from Houée-Levin et al. (2015) and Shiraiwa et al. (2012)) Subsequent intramolecular H-transfer initiated by irradiation decompose the protein and HONO is emitted (adapted from Bejan et al., 2006).

Fig. 2: Flow system and set-up: thin blue lines show the flow of the gas mixture, which direction is indicated by the grey triangles of the mass flow controllers (MFC). Nitrogen passes a heated water bath to humidify the gas and a HONO scrubber to eliminate any HONO impurities of the NO₂ supply. The overflow provides a stable pressure through the reaction tube and the detection unit. The dotted boxes (blue, green, orange) indicate the three different parts, the gas supply, reaction unit and detection unit.

Fig. 3: Light enhanced HONO formation from TNM-nitrated proteins (n-OVA: ND 12.5%, coating 21.5 $\mu\text{g cm}^{-2}$). Black squares indicate HONO formation via decomposition from nitrated proteins (without NO_2) while red squares indicate additional HONO formation via heterogeneous NO_2 conversion (20 ppb NO_2) at 50% RH (HONO is scaled to the HONO concentration measured without NO_2 and no light ($[\text{HONO}]_{\text{lights; NO}_2}/[\text{HONO}]_{\text{dark; NO}_2=0}$)).

Fig. 4: Light induced HONO formation on BSA. a) HONO formation under alternating dark and light conditions on BSA surface (22.5 $\mu\text{g cm}^{-2}$), yellow shaded areas indicate periods in which 7 VIS lamps were switched on (RH = 50%, $\text{NO}_2 = 20$ ppb); b) Dependency of HONO formation on radiation intensity at 20 ppb NO_2 and 50% RH (BSA = 31.4 $\mu\text{g cm}^{-2}$). The experiment started with 7 VIS lights switched on, sequentially decreasing the number of lights (red symbols, nominated 1-4), prior to apply the initial irradiance again (blue symbol, 5). HONO was scaled to the HONO concentration in darkness ($[\text{HONO}]_{\text{lights}}/[\text{HONO}]_{\text{dark}}$). Error bars indicate standard deviation of 20-30 min measurements, standard deviation of point 5 covers 2.75 h measurement.

Fig. 5: Comparison of HONO formation dependency on NO_2 at different organic surfaces. HONO concentrations are scaled to the HONO concentration at 20 ppb NO_2 ($[\text{HONO}]_{\text{NO}_2}/[\text{HONO}]_{\text{NO}_2=20\text{ppb}}$). Red square = BSA coating (16 $\mu\text{g cm}^{-2}$) at 161 W m^{-2} and 50% RH (this study), blue triangles pointing up = humic acid coating (8 $\mu\text{g cm}^{-2}$) at 162 W m^{-2} and 20% RH (Stemmler et al., 2006), dark blue triangles pointing down = humic acid aerosol with 100 nm diameter and a surface of 0.151 $\text{m}^2 \text{m}^{-3}$ at 26% RH and 1×10^{17} photons $\text{cm}^{-2} \text{s}^{-1}$ (Stemmler et al., 2007), black circles = gentisic acid coating (160-200 $\mu\text{g cm}^{-2}$) at 40-45% RH and light intensity similar as in the humic acid aerosol case (Sosedova et al., 2011), green diamonds = ortho-nitrophenol in gas phase (ppm level) illuminated with UV/VIS light. Dotted lines are exponential fittings of the measured data points and are guiding the eyes.

Fig. 6: HONO formation on three different BSA coating thicknesses, exposed to 20 ppb of NO_2 under illuminated conditions (7 VIS lamps). The HONO concentrations were scaled to reaction tube coverage (black: 100% of reaction tube was covered with BSA, blueish: 70% of tube was covered and red: 50% of tube was covered with BSA). The middle thick coating (22.46 $\mu\text{g cm}^{-2}$) was replicated and studied with different reaction times (cyan and blue triangle). Solid lines (with circles or triangles) present continuous measurements, when those are interrupted other conditions (e.g. light intensity, NO_2 concentration) prevailed. Dotted lines show interpolations and are for guiding the eyes. Arrows indicate the intervals in which the shown decay rates were determined. Error bars indicates standard deviations from 10-20 measuring points (5-10 min).

Fig. 7: Dependency of relative humidity on HONO formation. 25 ppb NO_2 was applied on BSA surface (17.5 $\mu\text{g cm}^{-2}$) either in darkness (blue triangle) or at 7 VIS lights (red star). HONO was scaled to HONO concentrations in darkness under dry conditions ($[\text{HONO}]_{\text{lights on-off; RH}}/[\text{HONO}]_{\text{dark; RH=0}}$). Dotted lines are for guiding the eyes.

Fig. 8: Extended measurements (20 h) of light-enhanced HONO formation on BSA (three coatings of 17.5 $\mu\text{g cm}^{-2}$) at 80% RH, 100 ppb NO_2 . HONO formation under VIS light is shown in red and orange, under UV/Vis light in blue. HONO decay rates [ppt h^{-1}] are shown with time periods (in brackets) in which they were calculated, suggesting a stable HONO formation after 4 hours. Right: zoom in on the first 2 hours. Straight lines (black, grey, light and dark blue) show the slopes of which $d[\text{HONO}]/dt$ were used in the kinetic studies.

References:

- Brigante, M., Cazoir, D., D'Anna, B., George, C., and Donaldson, D. J.: Photoenhanced uptake of NO_2 by pyrene solid films, *The Journal of Physical Chemistry A*, 112, 9503-9508, 10.1021/jp802324g, 2008.
- Selzle, K., Ackaert, C., Kampf, C. J., Kunert, A. T., Duschl, A., Oostingh, G. J., and Poschl, U.: Determination of nitration degrees for the birch pollen allergen Bet v 1, *Analytical and Bioanalytical Chemistry*, 405, 8945-8949, 10.1007/s00216-013-7324-0, 2013.

1 Light-induced protein nitration and degradation with HONO 2 emission

3 Hannah Meusel¹, Yasin Elshorbany², Uwe Kuhn¹, Thorsten Bartels-Rausch³, Kathrin Reinmuth-
4 Selzle¹, Christopher J. Kampf⁴, Guo Li¹, Xiaoxiang Wang¹, Jos Lelieveld⁵, Ulrich Pöschl¹,
5 Thorsten Hoffmann⁶, Hang Su^{1,7*}, Markus Ammann³, Yafang Cheng^{1,7*}

6 ¹ Max Planck Institute for Chemistry, Multiphase Chemistry Department, Mainz, Germany

7 ² NASA Goddard Space Flight Center, Greenbelt, Maryland, USA & Earth System Science Interdisciplinary Center,
8 University of Maryland, College Park, Maryland, USA

9 ³ Paul Scherer Institute, Villigen, Switzerland

10 ⁴ Johannes Gutenberg University, Institute for Organic Chemistry, Mainz, Germany

11 ⁵ Max Planck Institute for Chemistry, Atmospheric Chemistry Department, Mainz, Germany

12 ⁶ Johannes Gutenberg University, Institute for Inorganic and Analytical Chemistry, Mainz, Germany

13 ⁷ Institute for Environmental and Climate Research, Jinan University, Guangzhou, China

14 * Correspondence to: Y. Cheng (yafang.cheng@mpic.de) or H. Su (h.su@mpic.de)

15 **Abstract.** Proteins can be nitrated by air pollutants (NO₂), enhancing their allergenic potential. This work provides
16 insight into protein nitration and subsequent decomposition in the presence of solar radiation. We also investigated
17 light-induced formation of nitrous acid (HONO) from protein surfaces that were nitrated either online with
18 instantaneous gas phase exposure to NO₂ or offline by an efficient nitration agent (tetranitromethane, TNM). Bovine
19 serum albumin (BSA) and ovalbumin (OVA) were used as model substances for proteins. Nitration degrees of about
20 1% were derived applying NO₂ concentrations of 100 ppb under VIS/UV illuminated condition, while simultaneous
21 decomposition of (nitrated) proteins was also found during long-term (20h) irradiation exposure. **Measurements of**
22 **gas exchange measurements on TNM-nitrated proteins revealed that HONO can be formed and released even**
23 **without contribution of instantaneous heterogeneous NO₂ conversion. However, fumigation with NO₂ exposure** was
24 found to increase HONO emissions substantially. In particular, a strong dependence of HONO emissions on light
25 intensity, relative humidity (RH), NO₂ concentrations and the applied coating thickness were found. The 20 hours
26 long-term studies revealed sustained HONO formation, even if concentrations of the intact (nitrated) proteins were
27 too low to be detected after the gas exchange measurements. A reaction mechanism for the NO₂ conversion based on
28 the Langmuir-Hinshelwood kinetics is proposed.

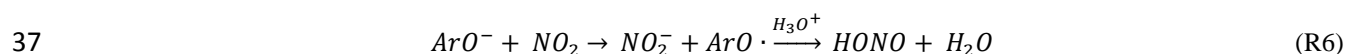
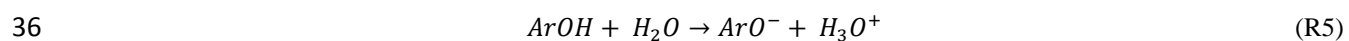
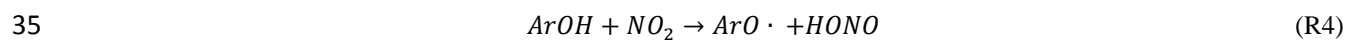
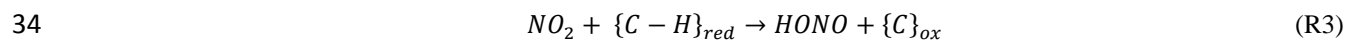
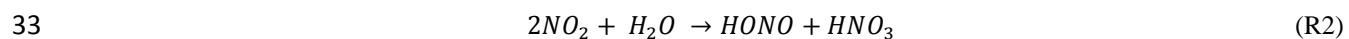
29 1 Introduction

30 Primary biological aerosols (PBA), or bioaerosols, including proteins, from different sources and with distinct
31 properties, are known to influence atmospheric cloud microphysics and public health (Lang-Yona et al., 2016;
32 D'Amato et al., 2007; Pummer et al., 2015). Bioaerosols represent a diverse subset of atmospheric particulate matter
33 that is directly emitted in form of active or dead organisms, or fragments, like bacteria, fungal spores, pollens,
34 viruses, and plant debris. Proteins are found ubiquitously in the atmosphere as part of these airborne, typically
35 coarse-size biological particles (diameter > 2.5 μm), but also in fine particulate matter (diameter < 2.5 μm)
36 associated with a host of different constituents such as polymers derived from biomaterials and proteins dissolved in

1 hydrometeors, mixed with fine dust and other particles (Miguel et al. 1999; Riediker et al., 2000; Zhang and
 2 Anastasio, 2003). Proteins contribute up to 5% of particle mass in airborne particles (Franze et al., 2003a; Staton et
 3 al., 2015; Menetrez et al., 2007) and are also found at surfaces of soils and plants. Proteins can be nitrated and are
 4 then likely to enhance allergic responses (Gruijthuisen et al., 2006). Nitrogen dioxide ($\bullet\text{NO}_2$) has emerged as an
 5 important biological reactant and has been shown to be capable of electron (or H atom) abstraction from the amino
 6 acid tyrosine (Tyr) to form TyrO \bullet in aqueous solutions (tyrosine phenoxyl radical, also called tyrosyl radical; Prütz et
 7 al. 1984 and 1985; Alfassi 1987; Houée-Lévin et al., 2015), which subsequently can be nitrated by a second NO_2
 8 molecule. Shiraiwa et al. (2012) observed nitration of protein aerosol, but not solely with NO_2 in the gasphase, and
 9 demonstrated that simultaneous O_3 exposure of airborne proteins in dark conditions can significantly enhance NO_2
 10 uptake and consequent protein nitration (3-nitrotyrosine formation) by way of direct O_3 -mediated formation of the
 11 TyrO \bullet intermediate. A connection between increased allergic diseases and elevated environmental pollution,
 12 especially traffic-related air pollution has been proposed (Ring et al., 2001). Tyrosine is one of the photosensitive
 13 amino acids and it is subject of direct and indirect photo-degradation under solar-simulated conditions (Boreen, et al.,
 14 2008), especially mediated by both UV-B (λ 280–320 nm) and UV-A (λ 320–400 nm) radiation (Houee-Levin et al.,
 15 2015; Bensasson et al., 1993). Direct light absorption or absorption by adjacent endogenous or exogenous
 16 chromophores and subsequent energy transfer results in an electronically-excited state of tyrosine (for details see
 17 Houée-Lévin et al. 2015 and references therein). If the triplet state of tyrosine is generated, it can undergo electron
 18 transfer reactions and deprotonation to yield TyrO \bullet (Fig.1, Bensasson 1993; Davies 1991; Berto et al., 2016).
 19 Regardless of how the tyrosyl radical is generated, it can be nitrated by reaction with NO_2 , but also hydroxylated or
 20 dimerized (Shiraiwa et al., 2012; Reinmuth-Selzle et al., 2014; Kampf et al., 2015).
 21 With respect to atmospheric chemistry, Bejan et al. (2006) have shown that photolysis of ortho-nitrophenols (as is
 22 the case for 3-nitrotyrosine) can generate nitrous acid (HONO). HONO is of great interest for atmospheric
 23 composition, as its photolysis forms OH radicals, being the key oxidant for degradation of most air pollutants in the
 24 troposphere (Levy, 1971). In the lower atmosphere, up to 30% of the primary OH radical production can be
 25 attributed to photolysis of HONO, especially during the early morning when other photochemical OH sources are
 26 still small (R1, Kleffmann et al., 2005; Alicke et al., 2002; Ren et al., 2006; Su et al., 2008; Meusel et al. 2016).



28 | HONO can be directly emitted by combustion of fossil fuels (Kurtenbach et al., 2001) or formed by gas phase
 29 reactions of NO and OH (the backwards reaction of R1) and heterogeneous reactions of NO_2 on wet surfaces
 30 according to R2. On carbonaceous surfaces (soot, phenolic compounds) HONO is formed via electron or H transfer
 31 reactions (R3 and R4-R6; Kalberer et al., 1999; Kleffmann et al., 1999; Gutzwiller et al., 2002; Aubin and Abbatt
 32 2007; Han et al., 2013; Arens et al., 2001, 2002; Ammann et al., 1998, 2005).



1 Previous atmospheric measurements and modeling studies have shown unexpected high HONO concentrations
2 during daytime, which can also contribute to aerosol formation through enhanced oxidation of precursor gases
3 (Elshorbany et al., 2014). Measured mixing ratios are typically about one order of magnitude higher than simulated
4 ones, and an additional source of 200-800 ppt h⁻¹ would be required to explain observed mixing ratios (Kleffmann et
5 al., 2005; Acker et al., 2006; Sörgel et al., 2011; Li et al., 2012; Su et al., 2008; Elshorbany et al., 2012; Meusel et al.,
6 2016) indicating that estimates of daytime HONO sources are still under debate. It was suggested that HONO arises
7 from the photolysis of nitric acid and nitrate or by heterogeneous photochemistry of NO₂ on organic substrates and
8 soot (Zhou et al., 2001; 2002 and 2003; Villena et al., 2011; Ramazan et al., 2004; George et al., 2005; Sosedova et
9 al., 2011; Monge et al., 2010; Han et al., 2016). Stemmler et al. (2006, 2007) found HONO formation on light-
10 activated humic acid, and field studies showed that HONO formation correlates with aerosol surface area, NO₂ and
11 solar radiation (Su et al., 2008; Reisinger, 2000; Costabile et al., 2010; Wong et al., 2012; Sörgel et al., 2015) and is
12 increased during foggy periods (Notholt et al., 1992). Another proposed source of HONO is the soil, where it has
13 been found to be co-emitted with NO by soil biological activities (Oswald et al., 2013; Su et al., 2011; Weber et al.,
14 2015).

15 In view of light-induced nitration of proteins and HONO formation by photolysis of nitro-phenols, light-enhanced
16 production of HONO on protein surfaces can be anticipated, which, to the best of our knowledge, has not been
17 studied before.

18 This work aims at providing insight into protein nitration, the atmospheric stability of the nitrated protein, and
19 respective formation of HONO from protein surfaces that were nitrated either offline in liquid phase prior to the gas
20 exchange measurements, or online with instantaneous gas phase exposure to NO₂, with particular emphasis on
21 environmental parameters like light intensity, relative humidity (RH) und NO₂ concentrations. Bovine serum
22 albumin (BSA), a globular protein with a molecular mass of 66.5 kDa and 21 tyrosine residues per molecule, was
23 chosen as a well-defined model substance for proteins. Nitrated ovalbumin (OVA) was used to study the light-
24 induced degradation of proteins that were nitrated prior to gas exchange measurements. This well-studied protein has
25 a molecular mass of 45 kDa and 10 tyrosine residues per molecule.

26 **2 Materials and methods**

27 **2.1 Protein preparation and analysis**

28 BSA (albumin from bovine serum, Cohn V fraction, lyophilized powder, ≥ 96%; Sigma Aldrich, St. Louis, Missouri,
29 USA) or nitrated OVA (ovalbumin) was solved in pure water (18.2MΩ cm) and coated onto the glass tube.

30 The nitration of ovalbumin (OVA) was described previously (Yang et al., 2010; Zhang et al., 2011). Briefly, OVA
31 (Grade V, A5503-5G, Sigma Aldrich, Germany) was dissolved in phosphate buffered saline PBS (P4417-50TAB,
32 Sigma Aldrich, Germany) to a concentration of 10 mg/ml. 50 µl tetranitromethane TNM (T25003-5G, Sigma
33 Aldrich, Germany) dissolved in methanol 4% (v/v) were added to a 2.5 ml aliquot of the OVA solution and stirred
34 for 180 min at room temperature. **Please note that TNM is toxic if swallowed, can cause skin, eye and respiration**
35 **irritation, is suspected to cause cancer and causes fire or explosion.** Size exclusion chromatography columns (PD-10

1 Sephadex G-25 M, 17-0851-01, GE Healthcare, Germany) were used for clean-up. The eluate was dried in a freeze
2 dryer and stored in a refrigerator at 4°C.

3 After the flow-tube-experiments (see below) the proteins were extracted with water from the tube and analyzed with
4 liquid chromatography (HPLC-DAD; Agilent Technologies 1200 series) according to Selzle et al. (2013). This
5 method provides a straightforward and efficient way to determine the nitration of proteins. Briefly, a monomerically
6 bound C18 column (Vydac 238TP, 250 mm×2.1 mm inner diameter, 5 µm particle size; Grace Vydac, Alltech) was
7 used for chromatographic separation. Eluents were 0.1 % (v/v) trifluoroacetic acid in water (LiChrosolv) (eluent A)
8 and acetonitrile (ROTISOLV HPLC Gradient Grade, Carl Roth GmbH + Co. KG, Germany) (eluent B). Gradient
9 elution was performed at a flow rate of 200 µL/min. ChemStation software (Rev. B.03.01, Agilent) was used for
10 system control and data analysis. For each chromatographic run, the solvent gradient started at 3% B followed by a
11 linear gradient to 90% B within 15 min, flushing back to 3% B within 0.2 min, and maintaining 3% B for additional
12 2.8 min. Column re-equilibration time was 5 min before the next run. Absorbance was monitored at wavelengths of
13 280 (tyrosine) and 357 nm (nitrotyrosine). The sample injection volume was 10-30 µL. Each chromatographic run
14 was repeated three times. The protein nitration degree, which is defined as the ratio of nitrated tyrosine to all tyrosine
15 residues, was determined by the method of Selzle et al. (2013). Native and un-treated BSA did not show any degree
16 of nitration.

17 2.2 Coated-wall flow tube system

18 Figure 2 shows a flowchart of the set-up of the experiment. NO₂ was provided in a gas bottle (1 ppm in N₂, Carbagas
19 AG, Grümligen, Switzerland). NO₂ was further diluted (mass flow controller, MFC3) with humidified pure nitrogen
20 to achieve NO₂ mixing ratios between 20 and 100 ppb. Impurities of HONO in the NO₂-gas cylinder were removed
21 by means of a HONO scrubber. The Na₂CO₃ trap was prepared by soaking 4mm firebrick in a saturated Na₂CO₃ in
22 50% ethanol / water solution and drying for 24 hours. The impregnated firebrick granules were put into a 0.8 cm
23 inner diameter and 15 cm long glass tube, which was closed by quartz wool plugs on both sides. A constant total
24 flow (1400 mL min⁻¹) was provided by means of another N₂ mass flow controller (MFC2) that compensated for
25 changes in NO₂ addition. Different fractions of total surface areas (50, 70 and 100%) of the reaction tube (50 cm x
26 0.81 cm i.d.) were coated with 2 mg BSA or nitrated OVA, respectively. Therefore 2 mg protein was dissolved in
27 600 µL pure water, injected into the tube and then gently dried in a low humidity N₂ flow (RH ~ 30-40%) with
28 continuous rotation of the tube. The coated reaction tube was exposed to the generated gas mixture and irradiated
29 with either (i) 1, 3 or 7 VIS lights (400-700 nm; L 15 W/954, lumilux de luxe daylight, Osram, Augsburg, Germany)
30 which is 0, 23, 69 or 161 W m⁻² respectively or (ii) 4 VIS and 3 UV lights (340-400 nm; UV-A, TL-D 15 W/10,
31 Philips, Hamburg, Germany).

32 An overview of the experiments performed during this study is shown in table 1. Light induced decomposition of
33 nitrated proteins was studied on OVA. Instantaneous NO₂ transformation and its light- and RH- dependence on
34 heterogeneous HONO formation were studied on BSA in short-term experiments. Extended studies on BSA were
35 performed to explore the persistence of the surface reactivity and respective catalytic effects.

36 A commercial long path absorption photometry instrument (LOPAP, QUMA) was used for HONO analysis. The
37 measurement technique was introduced by Heland et al. (2001). This wet chemical analytical method has an

1 unmatched low detection limit of 3-5 ppt with high HONO collection efficiency ($\geq 99\%$). HONO is continuously
2 trapped in a stripping coil flushed with an acidic solution of sulfanilamide. In a second reaction with n-(1-
3 naphthyl)ethylenediamine-dihydrochloride an azo dye is formed, whose concentration is determined by absorption
4 photometry in a long Teflon tubing. LOPAP has two stripping coils in series to reduce known interferences. In the
5 first stripping coil HONO is quantitatively collected. Due to the acidic stripping solution, interfering species are
6 collected less efficiently but in both channels. The true concentration of HONO is obtained by subtracting the
7 interferences quantified in the second channel from the total signal obtained in the first channel. The accuracy of the
8 HONO measurements was 10%, based on the uncertainties of liquid and gas flow, concentration of calibration
9 standard and regression of calibration.

10 The reagents were all high-purity-grade chemicals, i.e., hydrochloric acid (37 %, ACS reagent, Sigma Aldrich, St.
11 Louis, Missouri, USA), sulfanilamide (for analysis, $>99\%$; Sigma Aldrich) and N-(1-naphthyl)-ethylenediamine
12 dihydrochloride ($>98\%$; ACS reagent, Fluka by Sigma Aldrich). For calibration Titrisol® 1000 mg NO_2^- (NaNO_2 in
13 H_2O ; Merck) was diluted to 0.001 mg/L NO_2^- . For preparation of all solutions and for cleaning of the absorption
14 tubes 18M Ω H_2O was used.

15 NO_x concentrations were analyzed by means of a commercial chemiluminescence detector from EcoPhysics (CLD
16 77 AM, Duernten, Switzerland).

17 **3 Results and discussion**

18 **3.1 BSA nitration and degradation**

19 Nitrated proteins can ~~lead to a stronger trigger~~ allergic response. The nNitration of proteins can be enhanced by O_3
20 activation (in the dark). In the atmospheric environment, about half a day the time sunlight is present. What happens
21 with irradiated proteins when exposed to NO_2 ? Can they be nitrated efficiently? To investigate the degree of protein
22 nitration under illuminated conditions, BSA coated on the reaction tube ($17.5 \mu\text{g cm}^{-2}$) was exposed to 7 VIS lamps
23 (40% of a clear sky irradiance for a solar zenith of 48° ; Stemmler et al., 2006) and 100 ppb NO_2 at 70% RH. After 20
24 hours the BSA nitration degree (ND, concentration of nitrated tyrosine residues divided by the total concentration of
25 tyrosine residues) investigated by means of the HPLC-DAD method was $(1.0 \pm 0.1)\%$, significantly higher than the
26 ND of untreated BSA (0%). Introducing UV radiation (4 VIS plus 3 UV lamps) resulted in a slightly higher ND of
27 $(1.1 \pm 0.1)\%$. Note that no intact protein (nitrated and non-nitrated) could be detected by HPLC-DAD after another
28 20 hours of irradiation without NO_2 , indicating light induced decomposition of proteins. However, the applied
29 HPLC-DAD technique only detects (nitro-)tyrosine residues in proteins, and does not provide information about
30 protein fragments or single nitrated or non-nitrated tyrosine residues. Hence, proteins might have been decomposed
31 while tyrosine remains in its nitrated form, not detectable by our analysis method. Similarly, proteins (here: OVA)
32 that were nitrated with TNM in aqueous phase prior to coating ($21.5 \mu\text{g cm}^{-2}$) to an extent of 12.5% also decomposed
33 when illuminated about 6 hours (1-7 VIS lights; with and without 20 ppb NO_2). Thus the nitration of proteins by
34 light and NO_2 was confirmed, but with simultaneous gradual decomposition of the proteins. Effects of UV irradiation
35 (240-340 nm) on proteins containing aromatic amino acids were reviewed previously (Neves-Peterson et al., 2012).
36 It was shown that triplet state tryptophan and tyrosine can transfer electron to a nearby disulfide bridge to form the

1 tryptophan and tyrosine radical. The disulfide bridge could break leading to conformational changes in the protein
2 but not necessarily resulting in inactivation of the protein. In strong UV light (≈ 200 nm) the peptide bond could also
3 break (Nikogosyan and Görner, 1999).

4 Franze et al. (2005) analyzed a variety of natural samples (road dust, window dust and particulate matter PM_{2.5})
5 collected in the metropolitan area of Munich, containing 0.08-21 g/kg proteins, and revealed equivalent degrees of
6 nitration (EDN, concentration of nitrated protein divided by concentration of all proteins) between 0.01 and 0.1%
7 only. Such low nitration degree is in line with light induced decomposition of (nitrated) proteins. On the other hand,
8 an EDN up to 10% (average 5%) was found for BSA and birch pollen extract (BPE) exposed to Munich ambient air
9 for two weeks under dark conditions, with daily mean NO₂ (O₃) concentration of 17 to 50 ppb (7 to 43 ppb) in the
10 same study, possibly suggesting the deficiency of decomposition without being irradiated. BSA and OVA loaded on
11 syringe-filters and exposed to 200 ppb NO₂/O₃ for 6 days under dark conditions were nitrated to 6 and 8%,
12 respectively (Yang et al., 2010). Reinmuth-Selzle et al. (2014) found similar ND for major birch pollen allergen Bet
13 v 1 loaded on syringe-filters exposed to 80-470 ppb NO₂ and O₃. When exposed for 3-72 hours to NO₂/O₃ at RH <
14 92% the ND was 2-4%, while at condensing conditions (RH > 98%) the ND increased to 6% after less than one day
15 (19 hours). The ND of Bet v 1 was considerably increased to 22% for proteins solved in the aqueous phase (0.16 mg
16 mL⁻¹) when bubbling with a 120 ppb NO₂/O₃ gas mixture for a similar period of time (17 hours). Shiraiwa et al.
17 (2012) performed kinetic modelling and found that maximum 30% (conservative upper limit) of N-uptake on BSA
18 could be explained by NO₃ or N₂O₅, which are generated by the reaction of NO₂ and O₃, while overall nitration was
19 governed by an indirect mechanism in which a radical intermediate was formed by the reaction of BSA with ozone,
20 which then reacted with NO₂. On NaCl surface N-uptake was dominated by NO₃ and N₂O₅. Furthermore, NO₃
21 radicals, which in this study could be formed by photolysis of NO₂ (>410 nm, disproportionation of excited NO₂),
22 are not stable under the light conditions applied (400-700 nm) (Johnston et al., 1996). Therefore, in the present study
23 reactions with NO₃ were neglected. Photolysis of NO₂ forming NO (< 400 nm) can also be neglected (Gardner et al.,
24 1987; Roehl et al., 1994). A photolysis frequency for NO₂ of up to $5 \times 10^{-4} \text{ s}^{-1}$ under similar experimental light
25 conditions was determined by Stemmler et al., 2007. Other nitration methods, investigated by Reinmuth-Selzle et al.
26 (2014), e.g., nitration of Bet v 1 with peroxyxynitrite (ONOO⁻, formed by reaction of NO with O₂⁻) or TNM lead to ND
27 between 10 and 72% depending on reaction time, reagent concentration and temperature. Similarly, high NDs of 45-
28 50% were obtained by aqueous phase TNM nitration of BSA and OVA by Yang et al. (2010).

29 3.2 HONO formation

30 3.2.1 HONO formation from nitrated proteins

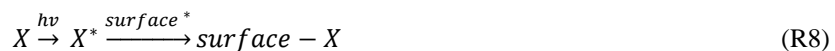
31 To study HONO emission from nitrated proteins, OVA was nitrated with TNM (see section 2.1) in liquid phase. The
32 nitrated OVA (2 mg; ND = 12.5%) was coated onto the reaction tube and exposed to VIS lights under either pure
33 nitrogen flow or 20 ppb NO₂ gas. Strong HONO emissions were found. ~~for OVA nitrated in the liquid phase prior to~~
34 ~~gas exchange measurements (ND = 12.5%).~~ A strong-high correlation between HONO emission and light intensity
35 was observed (50% RH; Fig. 3). Initially, we did not apply NO₂. Thus the observed HONO formation (up to 950 ppt)
36 originated from decomposing nitrated proteins rather than from heterogeneous conversion of NO₂. However, when
37 exposed to 20 ppb of NO₂ in dark conditions, HONO formation increased 4-fold (50 to 200 ppt), and about 2-fold

1 with 7 VIS lamps turned on (950 to 1800 ppt). After 7 hours of flow tube experiments (4.5 h irradiation with varying
 2 light intensities (0-1-3-7 lights) + 2.5 h irradiation/20 ppb NO₂ (7-3-0- lights)), no intact protein was found according
 3 to the analysis of HPLC-DAD.

4 As proteins can efficiently be nitrated by O₃ and NO₂ in polluted air (Franze et al., 2005, Shiraiwa et al., 2012;
 5 Reinmuth-Selzle et al. 2014), the emission of HONO from light-induced decomposing nitrated proteins could play an
 6 important role in the HONO budget. As proteins are nitrated at their tyrosine residues (at the ortho position to the OH
 7 group on the aromatic ring) the underlying mechanism of this HONO formation should be very similar to the HONO
 8 formation by photolysis of ortho-nitrophenols described by Bejan et al. (2006). This starts with a photo-induced
 9 hydrogen transfer from the OH group to the vicinal NO₂ group (Fig. 1), which leads to an excited intermediate from
 10 which HONO is eliminated subsequently.

11 3.2.2 Light dependency

12 To investigate HONO formation on unmodified BSA coating (31.4 μg cm⁻²) in dependence on light conditions, the
 13 radiation intensity (number of VIS lamps) was changed under otherwise constant conditions of exposure at 20 ppb
 14 NO₂ and 50% RH. Decreasing light intensity revealed a linearly decreasing trend in HONO formation from about
 15 1000 ppt to 140 ppt (red symbols in Fig. 4). After re-illumination to the initial high light intensity the HONO
 16 formation was reduced by 32% (blue symbol in Fig. 4). Stemmler et al. (2006) and Sosedova et al. (2011) also
 17 observed a similar saturation of HONO formation on humic acid, tannic and gentisic acid at higher light intensities.
 18 Stemmler et al. (2006) argued that surface sites activated for NO₂ heterogeneous conversion by light (R3) would
 19 become de-activated by competition with photo-induced oxidants (X*, R7-8), e.g., primary chromophores or electron
 20 donors are oxidized by surface*, which is in line with the observed decomposition of the native protein presented
 21 above.



24 In other studies the NO₂ uptake coefficient on soot, mineral dust, humic acid and other solid organic compounds
 25 similarly increased at increasing light intensities (George et al., 2005; Stemmler et al., 2007; Ndour et al., 2008;
 26 Monge et al., 2010; Han et al., 2016; Brigante et al., 2008). Note that the HONO yield (ratio of HONO formed to
 27 NO₂ lost) was found to be constant at light intensities in the range of 60-200 W m⁻² in the work of Han et al. (2016),
 28 but have shown a linear dependence on light for nitrated phenols (Bejan et al., 2006).

29 3.2.3 NO₂ dependency

30 At about 50% relative humidity and high illumination intensities (7 VIS lamps, ~161 W m⁻²), heterogeneous
 31 formation of HONO strongly correlated with the applied NO₂ concentration (Fig. 5). On a BSA surface of about 16.1
 32 μg cm⁻² (Tab. 1) the produced HONO concentration increased from 56 ppt at 20 ppb NO₂ to 160 ppt at 100 ppb NO₂.
 33 Only at a threshold NO₂ level well above those typically observed in natural environments (>>150 ppb) this
 34 increasing trend slowed down to some extent, indicative of saturation of active surface sites. A similar pattern of
 35 NO₂ dependence was also observed for light-induced HONO formation from humic acid (Stemmler et al., 2006) and

1 phenolic compounds like genticic and tannic acid (Sosedova et al., 2011) or polycyclic aromatic hydrocarbons
2 (Brigante et al., 2008), and for heterogeneous NO₂ conversion on soot under dark conditions (Stadler and Rossi,
3 2000; Salgado and Rossi, 2002; Arens et al., 2001).
4 For better comparison of the different studies the HONO concentration measured at different NO₂ concentrations
5 was normalized/scaled to the HONO concentration at 20 ppb NO₂ ([HONO]_{NO2}/[HONO]_{NO2=20ppb}) in Fig. 5, as
6 variable absolute amounts of HONO were found in different studies and matrices. A cease of the NO₂ dependency on
7 heterogeneous HONO formation can be assessed for most of the studies at NO₂ concentrations ≥ 200 ppb. A very
8 similar correlation (up to 40 ppb NO₂) was observed when NO₂ was applied additionally during the gas phase
9 photolysis of nitrophenols (fig. 5; Bejan et al., 2006). Even though the matrix (nitrophenols) and conditions
10 (illuminated) of the latter is comparable to the experiment presented here, for BSA no clear indication of saturation
11 was found up to 160 ppb of NO₂, pointing to a highly reactive surface of BSA for NO₂ under illuminated conditions.
12 As shown with R7 and R8, the concentration dependence depends on the competing channel R8, therefore, this is
13 strongly matrix dependent, both in terms of chemical and physical properties.

14 3.2.4 Impact of coating thickness

15 Strong differences in HONO concentrations were found for experiments with different coating thicknesses applying
16 otherwise similar conditions (20 ppb of NO₂, 7 VIS lamps and 50% RH). While only 55 ppt of HONO concentration
17 was observed for a shallow homogeneous coating of 16.1 μg cm⁻² (217.6 nm- thickness, see below) applied on the
18 whole length of the tube, up to 2 ppb were found for a thick (more uneven) coating of 31.44 μg cm⁻² (435.2 nm
19 thickness) covering only 50% of the tube (Fig. 6). Potential explanations are that thicker coating leads to (1) more
20 bulk reactions producing HONO, or (2) different morphologies, e.g., higher effective reaction surfaces. Exposing
21 (20%) different coated surface areas in the flow tube, potentially introduced bias comparing different data sets.
22 Emitted HONO might be re-adsorbed differently by proteins and glass surface. However, as the protein is slightly
23 acidic, a low uptake efficiency of HONO by BSA can be anticipated, which should not differ too much from the un-
24 covered glass tube surface (Syomin and Finlayson-Pitts, 2003). Accordingly, NO₂ uptake on glass is assumed to be
25 significantly lower than on proteins.

26 A strong increase in NO₂ uptake coefficients with increasing coating thickness was also observed for humic acid
27 coatings (Han et al., 2016). However, they found an upper threshold value of 2 μg cm⁻² of cover load (20 nm
28 absolute thickness, assuming a humic acid density of 1 g cm⁻³), above which uptake coefficients were found to be
29 constant. The authors also proposed that NO₂ can diffuse deeper into the coating and below 2 μg cm⁻² the full cover
30 depth would react with NO₂, respectively.

31 For proteins the number of molecules per monolayer depends on their orientation and respective layer thickness can
32 vary accordingly. One (dry, crystalline) BSA molecule has a volume of about 154 nm³ (Bujacz, 2012). In a flat
33 orientation (4.4 nm layer height, and a projecting area of 35 nm² per molecule) 3.64x10¹⁴ molecules (40.5 μg; 0.32
34 μg cm⁻²) of BSA are needed to form one complete monolayer in the flow tube (i.d. of 0.81 cm, 50 cm length, 100%
35 surface coating). Hence, the thinnest BSA coating applied in the experiment (16.1 μg cm⁻²) would consist of 50
36 monolayers revealing a total coating thickness of 217.6 nm, and the thickest BSA coating (31 μg cm⁻²) would have
37 99 monolayers and an absolute thickness of 435.1 nm. At the other extreme (non-flat) orientation, more BSA

1 molecules are needed to sustain one monolayer. With 21.7 nm² of projected area of one molecule and 7.1 nm
2 monolayer height, 5.86x10¹⁴ molecules of BSA are needed to form one complete monolayer in the flow tube. The
3 coatings would consist of between 31 (thinnest) and 61 (thickest) monolayers of BSA. With a flat orientation 1-2%
4 (number or weight) of BSA molecules would build the uppermost surface monolayer, whereas in an upright
5 molecule orientation 1.6-3.3% would be in direct contact with surface ambient air.

6 In the crystalline form several molecules of water stick tightly to BSA. As BSA is highly hygroscopic, more water
7 molecules are adsorbed at higher relative humidity. At 35% RH BSA is deliquesced (Mikhailov et al., 2004).
8 Therefore the above described number of monolayers and the absolute layer thickness are a lower bound estimate.

9 | In ~~conclusion~~vely, the thickness dependence on HONO formation is extremely complex. Activation and photolysis
10 of nitrated Tyr occurs throughout the BSA layer. The heterogeneous reaction of NO₂ may or may be not limited to
11 the surface depending on solubility and diffusivity of NO₂. Also the release of HONO may be limited by diffusion.
12 | The observed dependence on the coating thickness suggests the involvement of the bulk reactions, but the reactions
13 can happen in both, surface and bulk phase.

14 3.2.5 RH dependency

15 The dependence of HONO emission on relative humidity is shown in Fig. 7. Here about 25 ppb of NO₂ was applied
16 to a (not nitrated) BSA coated flow tube (17.5 µg cm⁻²) both in dark and illuminated conditions (7 VIS lights).
17 HONO formation scaled with relative humidity. Kleffmann et al. (1999) proposed that higher humidity inhibits the
18 self-reaction of HONO (2 HONO_(s,g) → NO₂ + NO + H₂O), which leads to higher HONO yield from heterogeneous
19 NO₂ conversion.

20 The RH dependence of HONO formation on proteins is different to other surfaces. For example, no influence of RH
21 has been observed for dark heterogeneous HONO formation on soot particles sampled on filters (Arens et al., 2001).

22 | No impact of humidity on NO₂ uptake coefficients on pyrene was detected (Brigante et al., 2008). For HONO
23 formation on tannic acid coatings (both at dark and irradiated conditions) a linear but relatively weak dependence has
24 been reported between 10 and 60% RH, while below 10% and above 60% RH the correlation between HONO
25 formation and RH was much stronger (Sosedova et al., 2011). Similar results were ~~observed~~ obtained for anthrabin
26 coatings by Arens et al. (2002). This type of dependence of HONO formation on phenolic surfaces on RH equals the
27 HONO formation on glass, following the BET water uptake isotherm of water on polar surfaces (Finnlayson-Pitts et
28 al., 2003; Summer et al., 2004). For humic acid surfaces the NO₂ uptake coefficients also weakly increased below
29 20% RH and were found to be constant between 20 and 60% (Stemmler et al., 2007).

30 While on solid matter chemical reactions are essentially confined to the surface rather than in the bulk, proteins can
31 adopt an amorphous solid or semisolid state, influencing the rate of heterogeneous reactions and multiphase
32 processes. Molecular diffusion in the non-solid phase affects the gas uptake and respective chemical transformation.
33 Shiraiwa et al. (2011) could show that the ozonolysis of amorphous protein is kinetically limited by bulk diffusion.
34 The reactive gas uptake exhibits a pronounced increase with relative humidity, which can be explained by a decrease
35 of viscosity and increase of diffusivity, as the uptake of water transforms the amorphous organic matrix from a
36 glassy to a semisolid state (moisture-induced phase transition). The viscosity and diffusivity of proteins depend
37 strongly on the ambient relative humidity because water can act as a plasticizer and increase the mobility of the

1 protein matrix (for details see Shiraiwa et al. 2011 and references therein). Shiraiwa et al. (2011) further showed that
2 the BSA phase changes from solid through semisolid to viscous liquid as RH increases, while trace gas diffusion
3 coefficients increased about 10 orders of magnitude. This way, characteristic times for heterogeneous reaction rates
4 can decrease from seconds to days as the rate of diffusion in semisolid phases can decrease by multiple orders of
5 magnitude in response to both low temperature (not investigated in here) and/or low relative humidity. Accordingly,
6 we propose that HONO formation rate depends on the condensed phase diffusion coefficients of NO₂ diffusing into
7 the protein bulk, HONO released from the bulk and mobility of excited intermediates.

8 **3.2.6 Long term exposure with NO₂ under irradiated conditions**

9 To study long-term effects of irradiation on HONO formation from proteins, flow tubes were coated with 2 mg BSA
10 ($17.5 \pm 0.4 \mu\text{g cm}^{-2}$; 90% of total length) and exposed to 100 ppb NO₂, at 80% RH at illuminated conditions for a
11 time period of up to 20 hours (Fig. 8). Samples illuminated with VIS light only (red and orange colored lines in Fig.
12 8) showed persistent HONO emissions over the whole measurement period. For reasons unknown, and even though
13 the observed HONO concentrations were within the expected range with regard to the applied NO₂ concentrations,
14 RH and cover characteristics, one sample (orange in Fig. 8) showed a sharp short-term increase in the initial phase
15 followed by respective decrease, not in line with all other samples (compare Fig. 6). However, after 4 hours both VIS
16 irradiated samples showed virtually constant HONO emissions (-3.8 and $+1.6 \text{ ppt h}^{-1}$, respectively). The sample
17 illuminated with UV/VIS light (3 UV and 4 VIS lamps) showed a sustained sharp increase in the first 4 hours,
18 followed by persistent and very stable (decay rate as low as -0.5 ppt h^{-1}) HONO emissions at an about 3-fold higher
19 level compared to samples irradiated with VIS only. **HONO formation by photolysis of (adsorbed) HNO₃ is assumed
20 to be insignificant in this study. With N₂ as carrier gas, gas phase reactions of NO₂ do not produce HNO₃. Even when
21 small amounts of HNO₃ would be formed by unknown heterogeneous reactions, photolysis of HNO₃ is only
22 significant at wavelengths < 350 nm, which is close to the lowest limit of the UV wavelength applied in this study.
23 Likewise, the respective photolysis frequency recently proposed by Laufs and Kleffmann (2016) of about 2.4×10^{-7}
24 s⁻¹ is very low.**

25 Integrating the 20 hour experiments, 9.23×10^{15} (4.6 ppb*h, VISa), 1.53×10^{16} (7.7 ppb*h, VISb) and 4.01×10^{16} (20
26 ppb*h, UV/VIS) molecules of HONO were produced. This means between 7.7×10^{13} and 3.3×10^{14} molecules of
27 HONO per cm² of BSA geometric surface were formed. With respect to the different experimental conditions
28 concerning cover thickness, RH, and NO₂ concentrations, this is in a similar order of magnitude as found for humic
29 acid (2×10^{15} molecules cm⁻² in 13 hours) by Stemmler et al. (2006).

30 If BSA acts like a catalytic **convertersurface** as in a Langmuir-Hinshelwood reaction each BSA molecule can react
31 several times with NO₂ to heterogeneously form HONO. As described in 3.1, BSA nitration is in competition with
32 NO₂ surface reactions and only a limited number of NO₂ molecules could react with BSA forming HONO via
33 nitration of proteins and subsequent decomposition of nitrated proteins. A BSA molecule contains 21 tyrosine
34 residues, which could react with NO₂. But even a strong nitration agent such as TNM is not capable of nitrating all
35 tyrosine residues and a mean nitration degree of 19% was found (Peterson et al., 2001; Yang et al., 2010), i.e., 4
36 tyrosine residues of one BSA molecule can be nitrated to form HONO. As 2 mg of BSA was applied for each flow
37 tube coating, a total of 1.8×10^{16} protein molecules can be inferred. In 20 hours of irradiating with VIS light 13-22%

1 of the accessible Tyr residues (4 each BSA molecule) would have been reacted. Irradiating with additional UV lights
 2 at least 56% of the tyrosine residues would have been nitrated and decomposed, respectively. But as NO₂ is a much
 3 weaker nitrating agent and nitration of only one tyrosine residue is probable (ND of BSA with O₃/NO₂ 6%; Yang et
 4 al., 2010) up to 85% BSA molecules would have been reacted when irradiated with VIS lights, and even more
 5 HONO molecules as coated BSA molecules would have been generated under UV/VIS light conditions. Other
 6 amino-acids of the protein like tryptophan or phenylalanine might also be nitrated but without formation of HONO
 7 (Goeschen et al., 2011). Hence, a contribution of heterogeneous conversion of NO₂ can be anticipated.

8 3.3 Kinetic studies

9 The experimental results (especially the stability over a long time) indicate that the formation of HONO from NO₂
 10 on protein surfaces likely underlies the Langmuir-Hinshelwood mechanism in which the protein would act as a
 11 catalytic ~~converter surface~~ (Fig. 9). The first step is the fast, reversible physical adsorption of NO₂ (k₁) and water
 12 followed by the slow conversion into HONO (eq.1 and eq.2). ~~In our experiments and in the atmosphere there is
 13 always sufficient water and for simplification we assume that the reaction rate only depends on NO₂.~~

$$14 \frac{d[NO_2]_s}{dt} = -k_1 * [NO_2]_g \quad \text{(eq.1)}$$

$$15 \frac{d[HONO]_s}{dt} = k_2 * [NO_2]_s \quad \text{(eq.2)}$$

16 ~~where index s and g indicate sorbed and gaseous state, respectively.~~

17 ~~From the experiments in which higher HONO concentrations were detected with higher light intensities we conclude
 18 that the heterogeneous conversion of NO₂ to HONO is light induced or a photochemical reaction. It was observed
 19 that the nitration of proteins is a competitive (side) reaction of the direct HONO formation (eq.2) but light induced
 20 decomposition of nitrated protein also produces HONO (eq.3).~~

$$21 \frac{d[HONO]_s}{dt} = k_4 * k_5 * [NO_2]_s \quad \text{(eq.3)}$$

22 ~~As these two processes cannot be discriminated by the observations presented here, we combine both reactions to
 23 formulate an overall formation equation (eq.4) with k' = k₂ + k₄*k₅~~

$$24 \frac{d[HONO]_s}{dt} = [HONO]_s + [HONO]_s = k' * [NO_2]_s \quad \text{(eq.4)}$$

25 There are two possible processes for the HONO formation. HONO is formed by heterogeneous NO₂ conversion (k₂)
 26 but also via nitration and decomposition of nitrated proteins (k₄, k₅). The final step of the mechanism is the release of
 27 the generated HONO into the air. Since proteins are in general slightly acidic, the desorption of HONO (k₃) should
 28 be fairly fast. ~~(eq.5)~~. Pseudo-first order kinetics are assumed for the reaction of NO₂ to HONO (Stemmler et al. 2007)
 29 and the reaction can be described as followed (eq.1).

$$30 \frac{d[HONO]_g}{dt} = k_3 * [HONO]_s \quad \text{(eq.5)}$$

31 ~~An effective formation rate of gaseous NO₂ to gaseous HONO k_{eff} was calculated according to eq.6.~~

$$32 \frac{d[HONO]_g}{dt} = k_{eff} * [NO_2]_g \quad \text{(eq.16)}$$

33 with k_{eff} = ~~k₁*k'*k₃~~ the effective pseudo-first order rate constant (for more detailed information check the
 34 supplement).

1 In this study, neither HONO nor NO₂ photolysis is considered, as the overlap of the applied UV/VIS or VIS range
2 (340-700 nm or 400-700 nm) and the HONO and NO₂ photolysis spectrum (<400 nm) is low. Furthermore, the
3 applied light intensity is lower compared to clear sky irradiance and the respective UV light is partly absorbed by the
4 reaction tube although quartz glass was used (transmission ~ 90%) and the photolysis frequency would decrease
5 down to 10⁻⁴ s⁻¹. Hence, the photolysis is assumed to be not significant.

6 In the first 5-10 min of the long-term experiments HONO increased (Fig. 8 – zoomed in range). This slope was taken
7 as d[HONO]_g/dt in eq.6. Effective rate constants between 1.48x10⁻⁶ s⁻¹ (VIS a) and 7.40x10⁻⁶ s⁻¹ (VIS b) were
8 calculated. When irradiating with VIS light only, the concentration of HONO was either constant or decreased for 2
9 h after this first 10 min. When irradiating with additional UV light, the HONO signal showed an enhancement in two
10 steps. In the first 10 min it was strongly increasing (1327 ppt h⁻¹) and then in the next hour it increased less with 170
11 ppt h⁻¹ prior to stabilization. Therefore two rate constants of 4.10x10⁻⁶ s⁻¹ and 5.2x10⁻⁷ s⁻¹ were obtained, respectively.
12 Reactive uptake coefficients for NO₂ were calculated according to Li et al. (2016). For both irradiation types the
13 uptake coefficient γ was in the range of 7x10⁻⁶ at the very beginning of each experiment. After a few minutes they
14 decreased to a mean of 1x10⁻⁷. The calculated k_{eff} values and uptake coefficient are in the same range and match the
15 NO₂ uptake coefficients on irradiated humic acid surfaces (coatings) and aerosols obtained by Stemmler et al. (2006
16 and 2007) which were in between 2x10⁻⁶ and 2x10⁻⁵ (coatings) and 1x10⁻⁶ and 6x10⁻⁶ (aerosols), depending on NO₂
17 concentrations and light intensities. Similar NO₂ uptake coefficients on humic acid were observed by Han et al.
18 (2016). George et al., (2005) reported about a two-fold increased NO₂ uptake coefficients for irradiated organic
19 substrates (benzophenone, catechol, anthracene) compared to dark conditions, in the order of (0.6-5)x10⁻⁶. NO₂
20 uptake coefficients on gentisic acid and tannic acid were in between (3.3-4.8)x10⁻⁷ (Sosedova et al., 2011), still
21 being higher than on fresh soot or dust (about 1x10⁻⁷; Monge et al., 2010; Ndour et al., 2008). The NO₂ uptake
22 coefficients on BSA in presence of O₃ (1x10⁻⁵, for 26 ppb NO₂ and 20 ppb O₃) published by Shiraiwa et al. (2012)
23 were somewhat higher than the values calculated here without O₃ but with light.

24 It was not possible to extract a set of parameters for a Langmuir Hinshelwood mechanism (like Langmuir
25 equilibrium constant, surface accommodation coefficient or second order rate constant) from the presented data. The
26 saturating behavior of photochemical HONO production may be due to either the adsorbed precursor on the surface
27 or due to a photochemical competition process, which also leads to a Lindemann-Hinshelwood type kinetic
28 expression (Minero, 1999).

29 ~~As proteins can efficiently be nitrated by O₃ and NO₂ in polluted air (Franze et al., 2005, Shiraiwa et al., 2012;
30 Reinmuth-Selzle et al. 2014), the emission of HONO from light induced decomposing nitrated proteins could play an
31 important role in the HONO budget. As proteins are nitrated at their tyrosine residues (at the ortho position to the OH
32 group on the aromatic ring) the underlying mechanism of this HONO formation should be very similar to the HONO
33 formation by photolysis of ortho nitrophenols described by Bejan et al. (2006). This starts with a photo induced
34 hydrogen transfer from the OH group to the vicinal NO₂ group (Fig. 1), which leads to an excited intermediate from
35 which HONO is eliminated subsequently.~~

36 4. Summary and Conclusion

1 Photochemical nitration of proteins accompanied by formation of HONO by (i) heterogeneous conversion of NO₂
2 and (ii) by decomposition of nitrated proteins was studied under relevant atmospheric conditions. NO₂ concentrations
3 ranged from 20 ppb (typical for urban regions in Europe and USA) up to 100 ppb (representative for highly polluted
4 industrial regions). The applied relative humidity of up to 80% and light intensities of up to 161 W/m² are common
5 on cloudy days. Under illuminated conditions very low nitration of proteins or even no native protein was observed,
6 indicating a light-induced decomposition of nitrated proteins to shorter peptides. These might still include nitrated
7 residues of which potential health effects are not yet known. An average effective rate constant of the total NO₂-
8 HONO conversion of $3.3 \times 10^{-6} \text{ s}^{-1}$ (for about 120 cm² of protein surface, layer thickness 240 nm and a layer volume
9 of 0.003 cm³; surface/volume ratio ~ 40000 cm⁻¹) or $8.25 \times 10^{-8} \text{ s}^{-1} \text{ per cm}^2 \text{ BSA layer}$ was obtained. At 20 ppb NO₂
10 ~~238 ppt h⁻¹ HONO would be formed. Projecting this to 1m² of pure BSA surface a formation of~~ HONO formation of
11 19.8 ppb ~~HONO~~ h⁻¹ m⁻² on a pure BSA surface could be estimated. While heterogeneous HONO formation of BSA
12 exposed to NO₂ revealed light saturation at intensities higher than 161 W m⁻², the HONO formation from previously
13 nitrated OVA was linearly increasing over the whole light intensity range investigated. The latter let assume even
14 higher HONO formation under sunny (clear sky) ambient atmospheric conditions. No data about representative
15 protein surface areas on atmospheric aerosol particles are available. However, the number and mass concentration of
16 primary biological aerosol particles such as pollen, fungal spores and bacteria, containing proteins, are in the range
17 of 10⁻¹⁰ m⁻³ and 10⁻³-1 μg m⁻³, respectively (Despres et al., 2012; Shiraiwa et al., 2012). Typical aerosol surface
18 concentrations in rural regions are about 100 μm² cm⁻³. Stemmler et al. (2007) estimated a HONO formation of 1.2
19 ppt h⁻¹ on pure humic acid aerosols in environmental conditions. As NO₂ uptake coefficients and HONO formation
20 rates on proteins are similar to humic acid, but only about 5% of the aerosol mass can be assumed to consist of
21 proteins, it can be anticipated that HONO formation on aerosol is not a significant HONO source in ambient
22 environmental settings. However, proteins on ground surfaces (soil, plants etc.) might play a more important role.
23 Accordingly, Stemmler et al. (2006 and 2007) suggested that NO₂ conversion on soil covered with humic acid would
24 be sufficient to explain missing HONO sources up to 700 ppt h⁻¹. Therefore it is difficult to estimate the importance
25 of HONO formation on protein surface and its contribution to the HONO budget. In many studies the calculated un-
26 known source strength of daytime HONO formation is within a range of about 200-800 ppt h⁻¹ (Kleffmann et al.,
27 2005; Acker et al., 2006; Li et al., 2012).

28 **Acknowledgment**

29 This study was supported by the Max Planck Society (MPG).

30 **References**

- 31 Acker, K., Moller, D., Wieprecht, W., Meixner, F. X., Bohn, B., Gilge, S., Plass-Dulmer, C., and Berresheim, H.:
32 Strong daytime production of OH from HNO₂ at a rural mountain site, Geophysical Research Letters, 33, 2006.
33 Alfassi, Z. B.: Selective Oxidation of Tyrosine Oxidation by NO₂ and ClO₂ at basic pH, Radiation Physics and
34 Chemistry, 29, 405-406, 1987.

1 Aliche, B., Platt, U., and Stutz, J.: Impact of nitrous acid photolysis on the total hydroxyl radical budget during the
2 Limitation of Oxidant Production/Pianura Padana Produzione di Ozono study in Milan, *Journal of Geophysical*
3 *Research-Atmospheres*, 107, 2002.

4 Ammann, M., Kalberer, M., Jost, D. T., Tobler, L., Rossler, E., Piguet, D., Gaggeler, H. W., and Baltensperger, U.:
5 Heterogeneous production of nitrous acid on soot in polluted air masses, *Nature*, 395, 157-160, 1998.

6 Ammann, M., Rossler, E., Strekowski, R., and George, C.: Nitrogen dioxide multiphase chemistry: Uptake kinetics
7 on aqueous solutions containing phenolic compounds, *Physical Chemistry Chemical Physics*, 7, 2513-2518,
8 10.1039/B501808K, 2005.

9 Arens, F., Gutzwiller, L., Baltensperger, U., Gaggeler, H. W., and Ammann, M.: Heterogeneous reaction of NO₂ on
10 diesel soot particles, *Environmental Science & Technology*, 35, 2191-2199, 10.1021/es000207s, 2001.

11 Arens, F., Gutzwiller, L., Gaggeler, H. W., and Ammann, M.: The reaction of NO₂ with solid anthracene (1,2,10-
12 trihydroxy-anthracene), *Physical Chemistry Chemical Physics*, 4, 3684-3690, 10.1039/B201713J, 2002.

13 Aubin, D. G., and Abbatt, J. P. D.: Interaction of NO₂ with hydrocarbon soot: Focus on HONO yield, surface
14 modification, and mechanism, *Journal of Physical Chemistry A*, 111, 6263-6273, 2007.

15 Bensasson RV, Land EJ, Truscott TG. Excited states and free radicals in biology and medicine. Oxford: Oxford
16 University Press; 1993.

17 Bejan, I., Abd El Aal, Y., Barnes, I., Benter, T., Bohn, B., Wiesen, P., and Kleffmann, J.: The photolysis of ortho-
18 nitrophenols: a new gas phase source of HONO, *Physical Chemistry Chemical Physics*, 8, 2028-2035, 2006.

19 Brigante, M., Cazoir, D., D'Anna, B., George, C., and Donaldson, D. J.: Photoenhanced uptake of NO₂ by pyrene
20 solid films, *The Journal of Physical Chemistry A*, 112, 9503-9508, 10.1021/jp802324g, 2008.

21 Bujacz, A.: Structures of bovine, equine and leporine serum albumin, *Acta Crystallographica Section D*, 68, 1278-
22 1289, doi:10.1107/S0907444912027047, 2012.

23 Costabile, F., Amoroso, A., and Wang, F.: Sub-mu m particle size distributions in a suburban Mediterranean area.
24 Aerosol populations and their possible relationship with HONO mixing ratios, *Atmospheric Environment*, 44,
25 5258-5268, 2010.

26 D'Amato, G., Cecchi, L., Bonini, S., Nunes, C., Annesi-Maesano, I., Behrendt, H., Liccardi, G., Popov, T., and Van
27 Cauwenberge, P.: Allergic pollen and pollen allergy in Europe, *Allergy*, 62, 976-990, 10.1111/j.1398-
28 9995.2007.01393.x, 2007.

29 Després, V., Huffman, J. A., Burrows, S. M., Hoose, C., Safatov, A., Buryak, G., Fröhlich-Nowoisky, J., Elbert, W.,
30 Andreae, M., Pöschl, U., and Jaenicke, R.: Primary biological aerosol particles in the atmosphere: a review,
31 *Tellus B: Chemical and Physical Meteorology*, 64, 15598, 10.3402/tellusb.v64i0.15598, 2012.

32 Elshorbany, Y. F., Steil, B., Brühl, C., and Lelieveld, J.: Impact of HONO on global atmospheric chemistry
33 calculated with an empirical parameterization in the EMAC model, *Atmos. Chem. Phys.*, 12, 9977-10000,
34 doi:10.5194/acp-12-9977-2012, 2012.

35 Elshorbany, Y.F., P. Crutzen, B. Steil, A. Pozzer, and J. Lelieveld, Global and regional impacts of HONO on the
36 chemical composition of clouds and aerosols, *Atmos. Chem. Phys.*, 14, 1167-1184, 2014.

1 Finlayson-Pitts, B. J., Wingen, L. M., Sumner, A. L., Syomin, D., and Ramazan, K. A.: The heterogeneous
2 hydrolysis of NO₂ in laboratory systems and in outdoor and indoor atmospheres: An integrated mechanism,
3 *Physical Chemistry Chemical Physics*, 5, 223-242, 10.1039/b208564j, 2003.

4 Franze, T., Krause, K., Niessner, R., and Poeschl, U.: Proteins and amino acids in air particulate matter, *Journal of*
5 *Aerosol Science*, 34, S777-S778, 2003.

6 Franze, T., Weller, M. G., Niessner, R., and Pöschl, U.: Protein nitration by polluted air, *Environmental Science &*
7 *Technology*, 39, 2005.

8 Gardner, E. P., Sperry, P. D., and Calvert, J. G.: Primary quantum yields of NO₂ photodissociation, *Journal of*
9 *Geophysical Research: Atmospheres*, 92, 6642-6652, 10.1029/JD092iD06p06642, 1987.

10 George, C., Strekowski, R. S., Kleffmann, J., Stemmler, K., and Ammann, M.: Photoenhanced uptake of gaseous
11 NO₂ on solid-organic compounds: a photochemical source of HONO?, *Faraday Discussions*, 130, 195-210,
12 2005.

13 Goeschen, C., Wibowo, N., White, J. M., and Wille, U.: Damage of aromatic amino acids by the atmospheric free
14 radical oxidant NO₃[radical dot] in the presence of NO₂[radical dot], N₂O₄, O₃ and O₂, *Organic &*
15 *Biomolecular Chemistry*, 9, 3380-3385, 10.1039/C0OB01186J, 2011.

16 Gruijthuijsen, Y. K., Grieshuber, I., Stoecklinger, A., Tischler, U., Fehrenbach, T., Weller, M. G., Vogel, L., Vieths,
17 S., Poeschl, U., and Duschl, A.: Nitration enhances the allergenic potential of proteins, *International Archives*
18 *of Allergy and Immunology*, 141, 265-275, 2006.

19 Han, C., Yang, W. J., Wu, Q. Q., Yang, H., and Xue, X. X.: Heterogeneous Photochemical Conversion of NO₂ to
20 HONO on the Humic Acid Surface under Simulated Sunlight, *Environmental Science & Technology*, 50, 5017-
21 5023, 2016.

22 Heland, J., Kleffmann, J., Kurtenbach, R., and Wiesen, P.: A new instrument to measure gaseous nitrous acid
23 (HONO) in the atmosphere, *Environmental Science & Technology*, 35, 3207-3212, 2001.

24 Houee-Levin, C., Bobrowski, K., Horakova, L., Karademir, B., Schoneich, C., Davies, M. J., and Spickett, C. M.:
25 Exploring oxidative modifications of tyrosine: An update on mechanisms of formation, advances in analysis
26 and biological consequences, *Free Radical Research*, 49, 347-373, 10.3109/10715762.2015.1007968, 2015.

27 Johnston, H. S., Davis, H. F., and Lee, Y. T.: NO₃ Photolysis Product Channels: Quantum Yields from Observed
28 Energy Thresholds, *The Journal of Physical Chemistry*, 100, 4713-4723, 10.1021/jp952692x, 1996.

29 Kalberer, M., Ammann, M., Arens, F., Gaggeler, H. W., and Baltensperger, U.: Heterogeneous formation of nitrous
30 acid (HONO) on soot aerosol particles, *Journal of Geophysical Research-Atmospheres*, 104, 13825-13832,
31 1999.

32 Kampf, C. J., Liu, F., Reinmuth-Selzle, K., Berkemeier, T., Meusel, H., Shiraiwa, M., and Pöschl, U.: Protein Cross-
33 Linking and Oligomerization through Dityrosine Formation upon Exposure to Ozone, *Environmental Science*
34 *& Technology*, 49, 10859-10866, 10.1021/acs.est.5b02902, 2015.

35 Kleffmann, J., H. Becker, K., Lackhoff, M., and Wiesen, P.: Heterogeneous conversion of NO₂ on carbonaceous
36 surfaces, *Physical Chemistry Chemical Physics*, 1, 5443-5450, 1999.

- 1 Kleffmann, J., Kurtenbach, R., Lorzer, J., Wiesen, P., Kalthoff, N., Vogel, B., and Vogel, H.: Measured and
2 simulated vertical profiles of nitrous acid - Part I: Field measurements, *Atmospheric Environment*, 37, 2949-
3 2955, 2003.
- 4 Kleffmann, J., Gavriloaiei, T., Hofzumahaus, A., Holland, F., Koppmann, R., Rupp, L., Schlosser, E., Siese, M., and
5 Wahner, A.: Daytime formation of nitrous acid: A major source of OH radicals in a forest, *Geophysical
6 Research Letters*, 32, 2005.
- 7 Kurtenbach, R., Becker, K. H., Gomes, J. A. G., Kleffmann, J., Lorzer, J. C., Spittler, M., Wiesen, P., Ackermann,
8 R., Geyer, A., and Platt, U.: Investigations of emissions and heterogeneous formation of HONO in a road traffic
9 tunnel, *Atmospheric Environment*, 35, 3385-3394, 2001.
- 10 Lang-Yona, N., Shuster-Meiseles, T., Mazar, Y., Yarden, O., and Rudich, Y.: Impact of urban air pollution on the
11 allergenicity of *Aspergillus fumigatus* conidia: Outdoor exposure study supported by laboratory experiments,
12 *Science of The Total Environment*, 541, 365-371, <http://dx.doi.org/10.1016/j.scitotenv.2015.09.058>, 2016.
- 13 Laufs, S., and J. Kleffmann: Investigations on HONO formation from photolysis of adsorbed HNO₃ on quartz glass
14 surfaces, *Phys. Chem. Chem. Phys.*, 18, 9616-9625, 2016.
- 15 Levy, H.: Normal Atmosphere: Large Radical and Formaldehyde Concentrations Predicted, *Science*, 173, 141-143,
16 1971.
- 17 Li, X., Brauers, T., Haeseler, R., Bohn, B., Fuchs, H., Hofzumahaus, A., Holland, F., Lou, S., Lu, K. D., Rohrer, F.,
18 Hu, M., Zeng, L. M., Zhang, Y. H., Garland, R. M., Su, H., Nowak, A., Wiedensohler, A., Takegawa, N., Shao,
19 M., and Wahner, A.: Exploring the atmospheric chemistry of nitrous acid (HONO) at a rural site in Southern
20 China, *Atmospheric Chemistry and Physics*, 12, 1497-1513, 2012.
- 21 Li, G., Su, H., Li, X., Kuhn, U., Meusel, H., Hoffmann, T., Ammann, M., Pöschl, U., Shao, M., and Cheng, Y.:
22 Uptake of gaseous formaldehyde by soil surfaces: a combination of adsorption/desorption equilibrium and
23 chemical reactions, *Atmos. Chem. Phys.*, 16, 10299-10311, [10.5194/acp-16-10299-2016](https://doi.org/10.5194/acp-16-10299-2016), 2016.
- 24 Menetrez, M. Y., Foarde, K. K., Dean, T. R., Betancourt, D. A., and Moore, S. A.: An evaluation of the protein mass
25 of particulate matter, *Atmospheric Environment*, 41, 8264-8274,
26 <http://dx.doi.org/10.1016/j.atmosenv.2007.06.021>, 2007.
- 27 Meusel, H., Kuhn, U., Reiffs, A., Mallik, C., Harder, H., Martinez, M., Schuladen, J., Bohn, B., Parchatka, U.,
28 Crowley, J. N., Fischer, H., Tomsche, L., Novelli, A., Hoffmann, T., Janssen, R. H. H., Hartogensis, O.,
29 Pikridas, M., Vrekoussis, M., Bourtsoukidis, E., Weber, B., Lelieveld, J., Williams, J., Pöschl, U., Cheng, Y.,
30 and Su, H.: Daytime formation of nitrous acid at a coastal remote site in Cyprus indicating a common ground
31 source of atmospheric HONO and NO, *Atmos. Chem. Phys.*, 16, 14475-14493, [10.5194/acp-16-14475-2016](https://doi.org/10.5194/acp-16-14475-2016),
32 2016.
- 33 Miguel, A. G., Cass, G. R., Glovsky, M. M., and Weiss, J.: Allergens in paved road dust and airborne particles,
34 *Environmental Science & Technology*, 33, 4159-4168, 1999.
- 35 Mikhailov, E., Vlasenko, S., Niessner, R., and Pöschl, U.: Interaction of aerosol particles composed of protein and
36 salts with water vapor: hygroscopic growth and microstructural rearrangement, *Atmos. Chem. Phys.*, 4, 323-
37 350, [10.5194/acp-4-323-2004](https://doi.org/10.5194/acp-4-323-2004), 2004.

1 | **Minero, C.: Kinetic analysis of photoinduced reactions at the water semiconductor interface, *Catal. Today*, 54, 205-**
2 | **216, 1999.**

3 | Monge, M. E., D'Anna, B., Mazri, L., Giroir-Fendler, A., Ammann, M., Donaldson, D. J., and George, C.: Light
4 | changes the atmospheric reactivity of soot, *Proceedings of the National Academy of Sciences of the United*
5 | *States of America*, 107, 6605-6609, 10.1073/pnas.0908341107, 2010.

6 | Ndour, M., D'Anna, B., George, C., Ka, O., Balkanski, Y., Kleffmann, J., Stemmler, K., and Ammann, M.:
7 | Photoenhanced uptake of NO₂ on mineral dust: Laboratory experiments and model simulations, *Geophysical*
8 | *Research Letters*, 35, 10.1029/2007gl032006, 2008.

9 | Neves-Petersen, M.T., Petersen, S., and Gajula, G.P. (2012): UV Light Effects on Proteins: From Photochemistry to
10 | Nanomedicine, *Molecular Photochemistry - Various Aspects*, Dr. Satyen Saha (Ed.), InTech, DOI:
11 | 10.5772/37947. Available from: [http://www.intechopen.com/books/molecular-photochemistry-various-](http://www.intechopen.com/books/molecular-photochemistry-various-aspects/uv-light-effects-on-proteins-from-photochemistry-to-nanomedicine)
12 | [aspects/uv-light-effects-on-proteins-from-photochemistry-to-nanomedicine](http://www.intechopen.com/books/molecular-photochemistry-various-aspects/uv-light-effects-on-proteins-from-photochemistry-to-nanomedicine).

13 | Nikogosyan, D. N., and Gorner, H.: Laser-induced photodecomposition of amino acids and peptides: extrapolation to
14 | corneal collagen, *IEEE Journal of Selected Topics in Quantum Electronics*, 5, 1107-1115,
15 | 10.1109/2944.796337, 1999.

16 | Notholt, J., Hjorth, J., and Raes, F.: Formation of HNO₂ on aerosol surfaces during foggy periods in the presence of
17 | NO and NO₂, *Atmospheric Environment Part a-General Topics*, 26, 211-217, 1992.

18 | Oswald, R., Behrendt, T., Ermel, M., Wu, D., Su, H., Cheng, Y., Breuninger, C., Moravek, A., Mouglin, E., Delon,
19 | C., Loubet, B., Pommerening-Roeser, A., Soergel, M., Poeschl, U., Hoffmann, T., Andreae, M. O., Meixner, F.
20 | X., and Trebs, I.: HONO Emissions from Soil Bacteria as a Major Source of Atmospheric Reactive Nitrogen,
21 | *Science*, 341, 1233-1235, 2013.

22 | Petersson, A.-S., Steen, H., Kalume, D. E., Caidahl, K., and Roepstorff, P.: Investigation of tyrosine nitration in
23 | proteins by mass spectrometry, *Journal of Mass Spectrometry*, 36, 616-625, 10.1002/jms.161, 2001.

24 | Prutz, W. A.: Tyrosine Oxidation by NO₂ in aqueous-solution, *Zeitschrift Fur Naturforschung C-a Journal of*
25 | *Biosciences*, 39, 725-727, 1984.

26 | Prutz, W. A., Monig, H., Butler, J., and Land, E. J.: Reactions of nitrogen dioxide in aqueous model systems –
27 | oxidation of tyrosine units in peptides and proteins, *Archives of Biochemistry and Biophysics*, 243, 125-134,
28 | 10.1016/0003-9861(85)90780-5, 1985.

29 | Pummer, B. G., Budke, C., Augustin-Bauditz, S., Niedermeier, D., Felgitsch, L., Kampf, C. J., Huber, R. G., Liedl,
30 | K. R., Loerting, T., Moschen, T., Schauerperl, M., Tollinger, M., Morris, C. E., Wex, H., Grothe, H., Pöschl, U.,
31 | Koop, T., and Fröhlich-Nowoisky, J.: Ice nucleation by water-soluble macromolecules, *Atmos. Chem. Phys.*,
32 | 15, 4077-4091, 10.5194/acp-15-4077-2015, 2015.

33 | Ramazan, K. A., Syomin, D., and Finlayson-Pitts, B. J.: The photochemical production of HONO during the
34 | heterogeneous hydrolysis of NO₂, *Physical Chemistry Chemical Physics*, 6, 3836-3843, 2004.

35 | Reinmuth-Selzle, K., Ackaert, C., Kampf, C. J., Samonig, M., Shiraiwa, M., Kofler, S., Yang, H., Gadermaier, G.,
36 | Brandstetter, H., Huber, C. G., Duschl, A., Oostingh, G. J., and Pöschl, U.: Nitration of the Birch Pollen
37 | Allergen Bet v 1.0101: Efficiency and Site-Selectivity of Liquid and Gaseous Nitrating Agents, *Journal of*
38 | *Proteome Research*, 13, 1570-1577, 2014.

1 Reisinger, A. R.: Observations of HNO₂ in the polluted winter atmosphere: possible heterogeneous production on
2 aerosols, *Atmospheric Environment*, 34, 3865-3874, 2000.

3 Ren, X., Brune, W. H., Olinger, A., Metcalf, A. R., Simpas, J. B., Shirley, T., Schwab, J. J., Bai, C., Roychowdhury,
4 U., Li, Y., Cai, C., Demerjian, K. L., He, Y., Zhou, X., Gao, H., and Hou, J.: OH, HO₂, and OH reactivity
5 during the PMTACS-NY Whiteface Mountain 2002 campaign: Observations and model comparison, *Journal of*
6 *Geophysical Research-Atmospheres*, 111, 2006.

7 Riediker, Koller, and Monn: Differences in size selective aerosol sampling for pollen allergen detection using high-
8 volume cascade impactors, *Clinical & Experimental Allergy*, 30, 867-873, 10.1046/j.1365-2222.2000.00792.x,
9 2000.

10 Ring, J., Kramer, U., Schafer, T., and Behrendt, H.: Why are allergies increasing?, *Current Opinion in Immunology*,
11 13, 701-708, 2001.

12 Roehl, C. M., Orlando, J. J., Tyndall, G. S., Shetter, R. E., Vazquez, G. J., Cantrell, C. A., and Calvert, J. G.:
13 Temperature Dependence of the Quantum Yields for the Photolysis of NO₂ Near the Dissociation Limit, *The*
14 *Journal of Physical Chemistry*, 98, 7837-7843, 10.1021/j100083a015, 1994.

15 Salgado, M. S., and Rossi, M. J.: Flame soot generated under controlled combustion conditions: Heterogeneous
16 reaction of NO₂ on hexane soot, *International Journal of Chemical Kinetics*, 34, 620-631, 10.1002/kin.10091,
17 2002.

18 Selzle, K.; Ackaert, C.; Kampf, C. J., et al., Determination of nitration degrees for the birch pollen allergen Bet v 1.
19 *Analytical and Bioanalytical Chemistry* 2013, 405 (27), 8945-8949.

20 Shiraiwa, M., Ammann, M., Koop, T., and Pöschl, U.: Gas uptake and chemical aging of semisolid organic aerosol
21 particles, *Proceedings of the National Academy of Sciences*, 108, 11003-11008, 10.1073/pnas.1103045108,
22 2011.

23 Shiraiwa, M., Selzle, K., Yang, H., Sosedova, Y., Ammann, M., and Poeschl, U.: Multiphase Chemical Kinetics of
24 the Nitration of Aerosolized Protein by Ozone and Nitrogen Dioxide, *Environmental Science & Technology*,
25 46, 6672-6680, 2012.

26 Sörgel, M., Regelin, E., Bozem, H., Diesch, J. M., Drewnick, F., Fischer, H., Harder, H., Held, A., Hosaynali-Beygi,
27 Z., Martinez, M., and Zetzsch, C.: Quantification of the unknown HONO daytime source and its relation to
28 NO₂, *Atmospheric Chemistry and Physics*, 11, 10433-10447, 2011.

29 Sörgel, M., Trebs, I., Wu, D., and Held, A.: A comparison of measured HONO uptake and release with calculated
30 source strengths in a heterogeneous forest environment, *Atmos. Chem. Phys.*, 15, 9237-9251, 10.5194/acp-15-
31 9237-2015, 2015.

32 Sosedova, Y., Rouviere, A., Bartels-Rausch, T., and Ammann, M.: UVA/Vis-induced nitrous acid formation on
33 polyphenolic films exposed to gaseous NO₂, *Photochemical & Photobiological Sciences*, 10, 1680-1690, 2011.

34 Stadler, D., and Rossi, M. J.: The reactivity of NO₂ and HONO on flame soot at ambient temperature: The influence
35 of combustion conditions, *Physical Chemistry Chemical Physics*, 2, 5420-5429, 10.1039/b005680o, 2000.

36 Staton, S. J. R., Woodward, A., Castillo, J. A., Swing, K., and Hayes, M. A.: Ground level environmental protein
37 concentrations in various ecuadorian environments: Potential uses of aerosolized protein for ecological
38 research, *Ecological Indicators*, 48, 389-395, <http://dx.doi.org/10.1016/j.ecolind.2014.08.036>, 2015.

1 Stemmler, K., Ammann, M., Donders, C., Kleffmann, J., and George, C.: Photosensitized reduction of nitrogen
2 dioxide on humic acid as a source of nitrous acid, *Nature*, 440, 195-198, 2006.

3 Stemmler, K., Ndour, M., Elshorbany, Y., Kleffmann, J., D'Anna, B., George, C., Bohn, B., and Ammann, M.: Light
4 induced conversion of nitrogen dioxide into nitrous acid on submicron humic acid aerosol, *Atmospheric*
5 *Chemistry and Physics*, 7, 4237-4248, 2007.

6 Su, H., Cheng, Y. F., Shao, M., Gao, D. F., Yu, Z. Y., Zeng, L. M., Slanina, J., Zhang, Y. H., and Wiedensohler, A.:
7 Nitrous acid (HONO) and its daytime sources at a rural site during the 2004 PRIDE-PRD experiment in China,
8 *Journal of Geophysical Research-Atmospheres*, 113, 2008b.

9 Su, H., Cheng, Y., Oswald, R., Behrendt, T., Trebs, I., Meixner, F. X., Andreae, M. O., Cheng, P., Zhang, Y., and
10 Poeschl, U.: Soil Nitrite as a Source of Atmospheric HONO and OH Radicals, *Science*, 333, 1616-1618, 2011.

11 Sumner, A. L., Menke, E. J., Dubowski, Y., Newberg, J. T., Penner, R. M., Hemminger, J. C., Wingen, L. M.,
12 Brauers, T., and Finlayson-Pitts, B. J.: The nature of water on surfaces of laboratory systems and implications
13 for heterogeneous chemistry in the troposphere, *Physical Chemistry Chemical Physics*, 6, 604-613,
14 10.1039/B308125G, 2004.

15 Syomin, D. A. and Finlayson-Pitts, B. J.: HONO decomposition on borosilicate glass surfaces: implications for
16 environmental chamber studies and field experiments, *Physical Chemistry Chemical Physics*, 5, 5236-5242,
17 2003.

18 Villena, G., Wiesen, P., Cantrell, C. A., Flocke, F., Fried, A., Hall, S. R., Hornbrook, R. S., Knapp, D., Kosciuch, E.,
19 Mauldin, R. L., McGrath, J. A., Montzka, D., Richter, D., Ullmann, K., Walega, J., Weibring, P., Weinheimer,
20 A., Staebler, R. M., Liao, J., Huey, L. G., and Kleffmann, J.: Nitrous acid (HONO) during polar spring in
21 Barrow, Alaska: A net source of OH radicals?, *Journal of Geophysical Research: Atmospheres*, 116, n/a-n/a,
22 2011.

23 Vogel, B., Vogel, H., Kleffmann, J., and Kurtenbach, R.: Measured and simulated vertical profiles of nitrous acid -
24 Part II. Model simulations and indications for a photolytic source, *Atmospheric Environment*, 37, 2957-2966,
25 2003.

26 Weber, B., Wu, D., Tamm, A., Ruckteschler, N., Rodriguez-Caballero, E., Steinkamp, J., Meusel, H., Elbert, W.,
27 Behrendt, T., Soergel, M., Cheng, Y., Crutzen, P. J., Su, H., and Poeschi, U.: Biological soil crusts accelerate
28 the nitrogen cycle through large NO and HONO emissions in drylands, *Proceedings of the National Academy*
29 *of Sciences of the United States of America*, 112, 15384-15389, 2015.

30 Wong, K. W., Tsai, C., Lefter, B., Haman, C., Grossberg, N., Brune, W. H., Ren, X., Luke, W., and Stutz, J.: Daytime
31 HONO vertical gradients during SHARP 2009 in Houston, TX, *Atmospheric Chemistry and Physics*, 12, 635-
32 652, 2012.

33 Yang, H.; Zhang, Y. Y.; Pöschl, U., Quantification of nitrotyrosine in nitrated proteins. *Analytical and Bioanalytical*
34 *Chemistry* 2010, 397 (2), 879-886.

35 Zhang, Y. Y.; Yang, H.; Pöschl, U., Analysis of nitrated proteins and tryptic peptides by HPLC-chip-MS/MS: site-
36 specific quantification, nitration degree, and reactivity of tyrosine residues. *Analytical and Bioanalytical*
37 *Chemistry* 2011, 399 (1), 459-471.

1 Zhang, Q., and Anastasio, C.: Free and combined amino compounds in atmospheric fine particles (PM_{2.5}) and fog
 2 waters from Northern California, *Atmospheric Environment*, 37, 2247-2258, 2003.

3 Zhou, X. L., Beine, H. J., Honrath, R. E., Fuentes, J. D., Simpson, W., Shepson, P. B., and Bottenheim, J. W.:
 4 Snowpack photochemical production of HONO: a major source of OH in the Arctic boundary layer in
 5 springtime, *Geophysical Research Letters*, 28, 4087-4090, 2001.

6 Zhou, X. L., Civerolo, K., Dai, H. P., Huang, G., Schwab, J., and Demerjian, K.: Summertime nitrous acid chemistry
 7 in the atmospheric boundary layer at a rural site in New York State, *Journal of Geophysical Research-*
 8 *Atmospheres*, 107, 2002a.

9 Zhou, X. L., Gao, H. L., He, Y., Huang, G., Bertman, S. B., Civerolo, K., and Schwab, J.: Nitric acid photolysis on
 10 surfaces in low-NO_x environments: Significant atmospheric implications, *Geophysical Research Letters*, 30,
 11 2003.

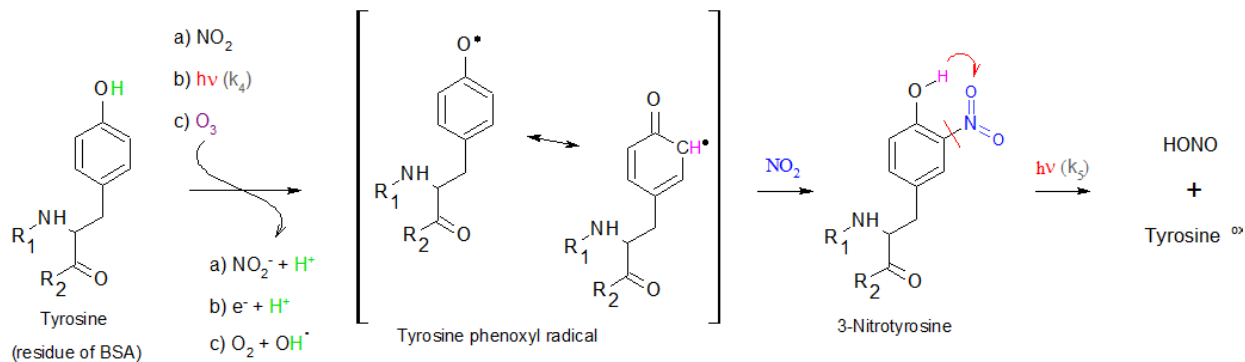
12

13 Tables and Figures

14 **Tab 1: Details on the different experiments, aims and experimental conditions (coating, applied NO₂ concentration,**
 15 **number of lights switched on, relative humidity and time for each exposure step):**

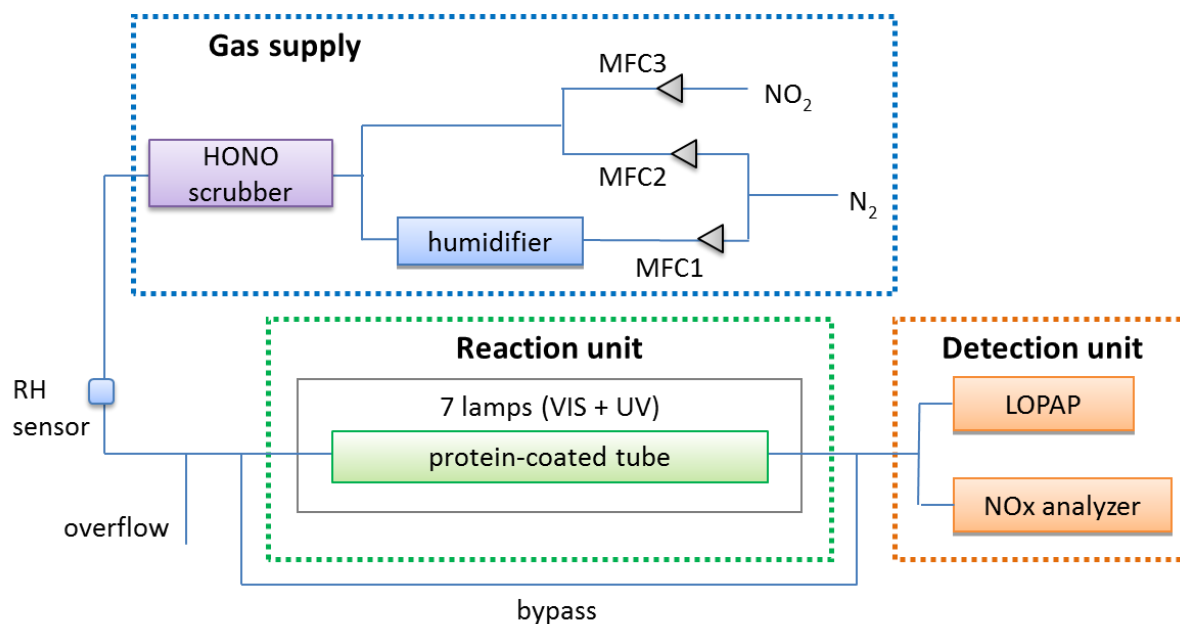
	Coating density (number of monolayers NML _f , thickness)	NO ₂ [ppb]	no. of lamps	RH [%]	time per step [h]
A light induced decomposition of nitrated protein and HONO formation					
1 light and NO ₂ dependency	n-OVA 21.5 ± 0.8 µg cm ⁻² (68 NML _f , 298.05 nm)	0-20	0-1-3-7 VIS	50	1
B heterogeneous NO₂ transformation on BSA					
2 NO ₂ dependency	BSA 16.1±0.4 µg cm ⁻² (50 NML _f , 217.6 nm)	0-20-40-60- 100	7 VIS	50	0.5-1
3 light dependency	BSA 31.4±1.4 µg cm ⁻² (99 NML _f , 435.2 nm)	20	0-1-3-7 VIS	50	0.5-1
4 coating thickness	BSA 16.1±0.4 µg cm ⁻² (50 NML _f , 217.6 nm), 22.5±0.8 µg cm ⁻² (71 NML _f , 310.8 nm), 31.4±1.4 µg cm ⁻² (99 NML _f , 435.2 nm)	20	7 VIS		0.5-3
5 RH dependency	BSA 17.5±0.4 µg cm ⁻² (55 NML _f , 241.7 nm)	25	0-7VIS	0-50-80	0.25-1
6 time effect	BSA 17.5±0.4 µg cm ⁻²	100	7 VIS	75	20
7 time effect	BSA 17.5±0.4 µg cm ⁻²	100	4 VIS + 3 UV	75	20

16 NML_f numbers of monolayers in flat orientation
 17
 18
 19
 20
 21



7
8
9
10
11

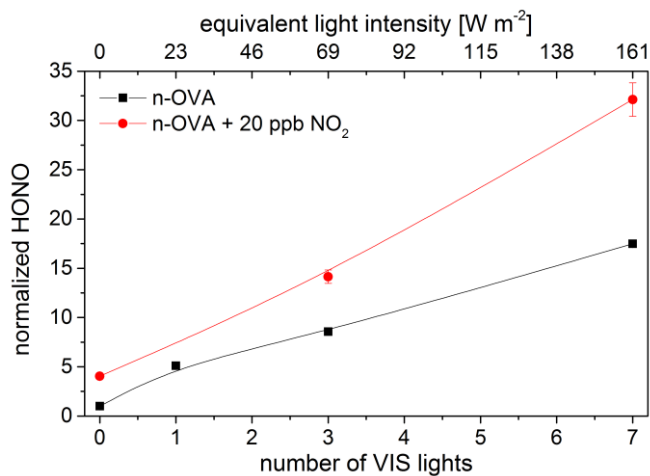
Fig. 1: Overview on possible reaction mechanisms of atmospheric BSA nitration and subsequent HONO emission. The tyrosine phenoxyl radical intermediate is either formed by the reaction of tyrosine with a) NO_2 , b) light or c) ozone. A second reaction with NO_2 (formation of the tyrosine phenoxyl radical and following NO_2 addition to forms 3-nitrotyrosine (was adapted from Houé-Levin et al. (2015) and Shiraiwa et al. (2012)); Subsequent intramolecular H-transfer initiated by irradiation decompose the protein and HONO is emitted (adapted from Bejan et al., 2006).



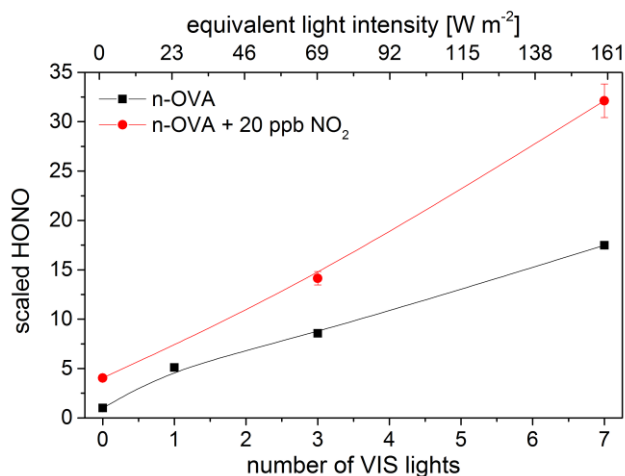
18
19
20
21
22

Fig. 2: Flow system and set-up; MFC = mass flow controller - thin blue lines show the flow of the gas mixture, which direction is indicated by the grey triangles of the mass flow controllers (MFC). Nitrogen passes a heated water bath to humidify the gas and a HONO scrubber to eliminate any HONO impurities of the NO_2 supply. The overflow provides maintains a stable constant pressure through the reaction tube and the detection unit. The dotted boxes (blue, green, orange) indicate the three different parts, the gas supply, reaction unit and detection unit.

1
2



3



4

5 **Fig. 3: Light enhanced HONO formation from TNM-nitrated proteins -nitrated in the liquid phase prior to the flow tube**
6 **experiments (n-OVA: ND 12.5%, coating 21.5 μg cm⁻²). with and without** Black squares indicate HONO formation via
7 **decomposition from nitrated proteins (without NO₂) while red squares indicate additional HONO formation via**
8 **heterogeneous NO₂ conversion in the purging air (20 ppb NO₂) at 50% RH (HONO is normalized**
9 **scaled to the HONO concentration measured without NO₂ and no light ([HONO]_{lights; NO2}/[HONO]_{dark; NO2=0})).**

10
11
12
13
14

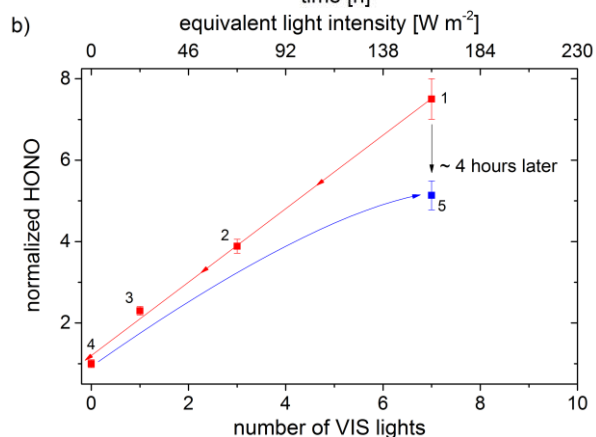
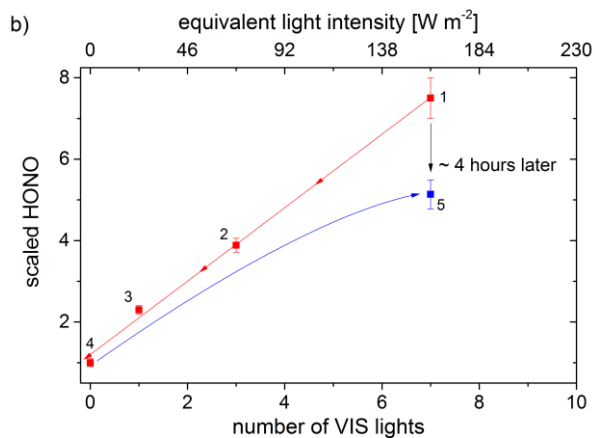
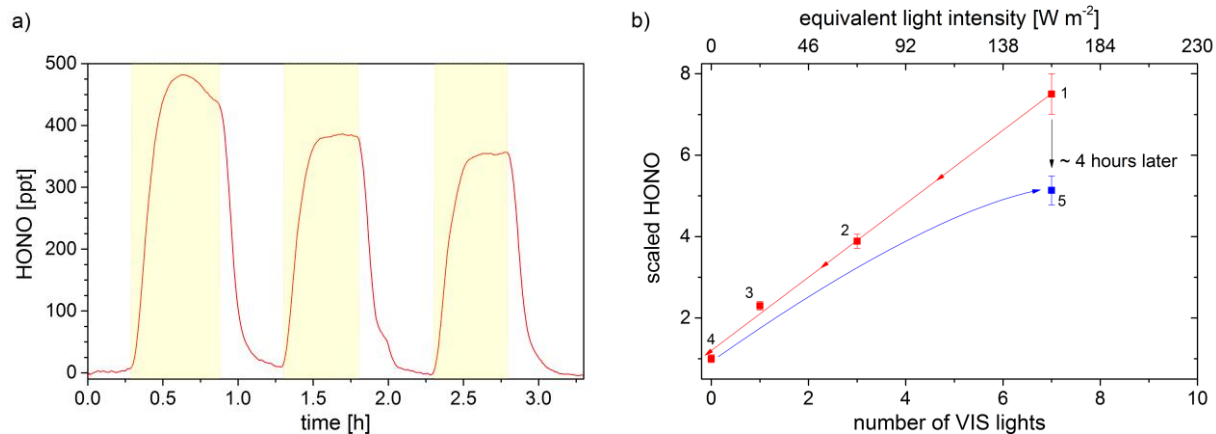
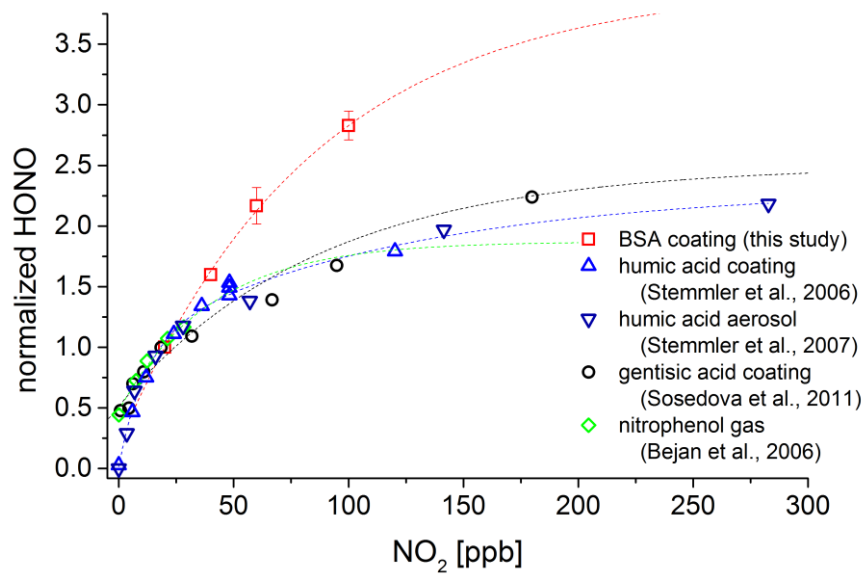
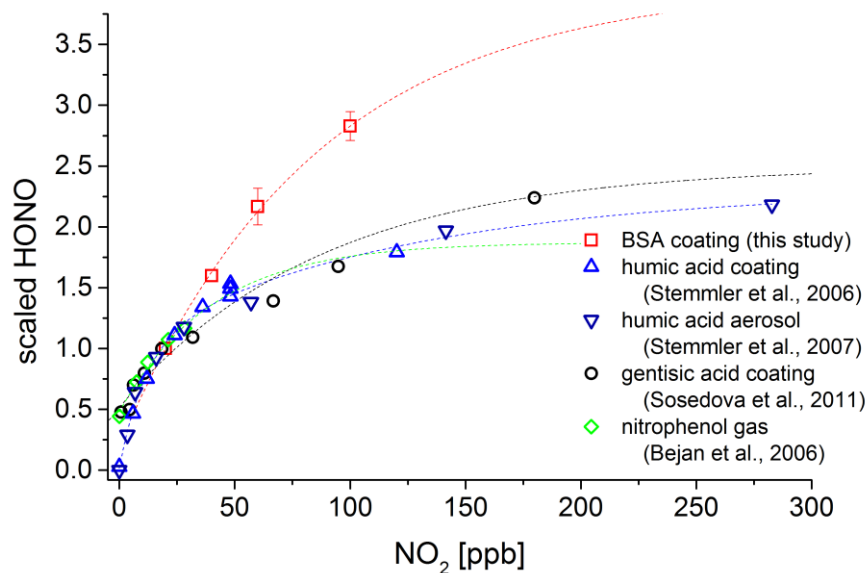


Fig. 4: Light induced HONO formation on BSA. a) Light enhancement of HONO formation under alternating dark and light conditions on BSA surface ($22.5 \mu\text{g cm}^{-2}$), yellow shaded areas indicate periods in which 7 VIS lamps were switched on (RH = 50%, $\text{NO}_2 = 20 \text{ ppb}$); b) Dependency of HONO formation on radiation intensity at 20 ppb NO_2 and 50% RH (BSA = $31.4 \mu\text{g cm}^{-2}$). The experiment started with 7 VIS lights switched on, sequentially decreasing the number of lights (red symbols, nominated 1-4), prior to apply the initial irradiance again (blue symbol, 5). HONO was normalized/scaled to the HONO concentration in darkness ($[\text{HONO}]_{\text{lights}}/[\text{HONO}]_{\text{dark}}$). Error bars indicate standard deviation of 20-30 min measurements, standard deviation of point 5 covers 2.75 h measurement.



1

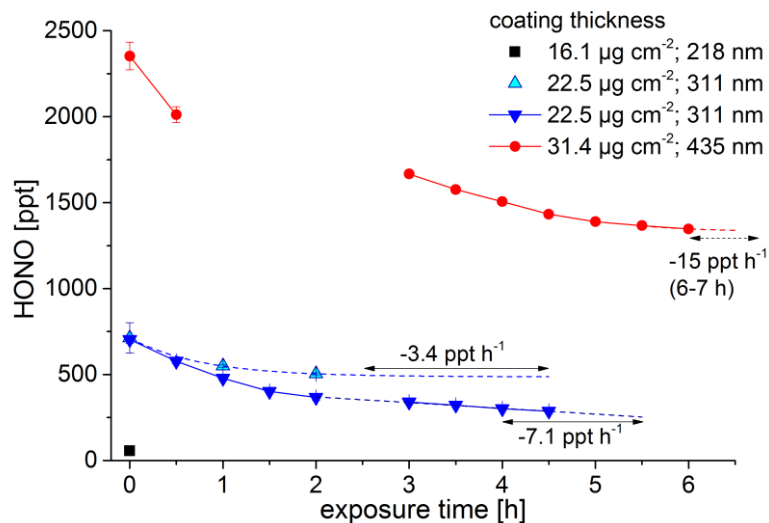
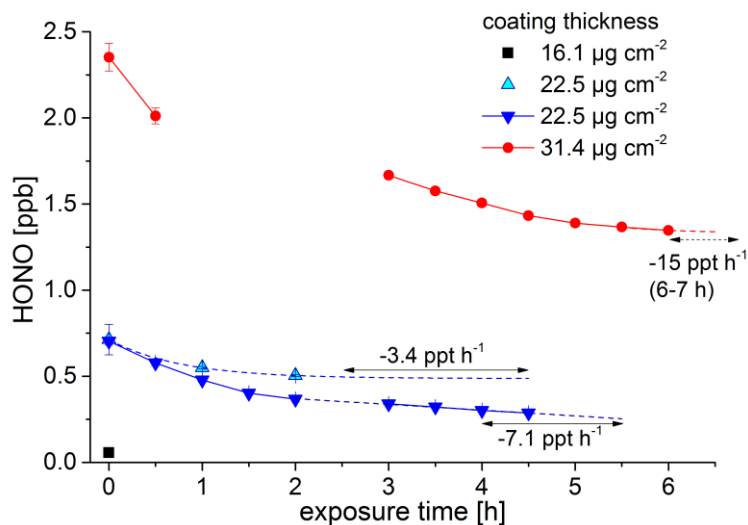


2

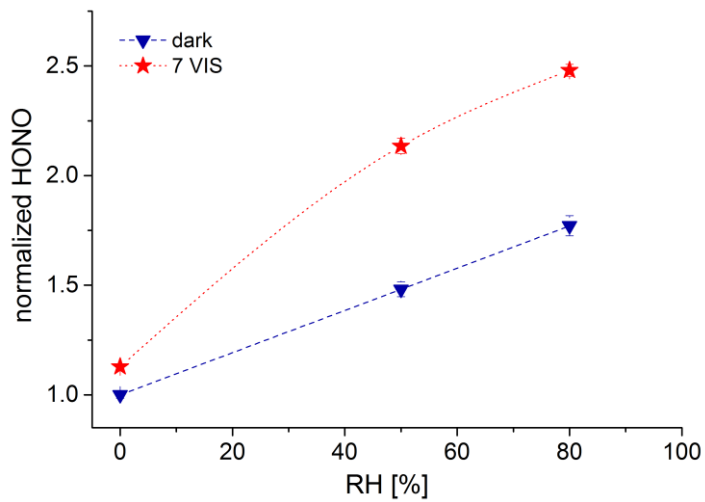
3 Fig. 5: Comparison of HONO formation dependency on NO_2 at different organic surfaces. HONO concentrations are
 4 **normalized** scaled to the HONO concentration at 20 ppb NO_2 ($[\text{HONO}]_{\text{NO}_2}/[\text{HONO}]_{\text{NO}_2=20\text{ppb}}$). Red square = BSA coating
 5 ($16 \mu\text{g cm}^{-2}$) at 161 W m^{-2} and 50% RH (this study), blue triangles pointing up = humic acid coating ($8 \mu\text{g cm}^{-2}$) at 162 W
 6 m^{-2} and 20% RH (Stemmler et al., 2006), dark blue triangles pointing down = humic acid aerosol with 100 nm diameter
 7 and a surface of $0.151 \text{ m}^2 \text{ m}^{-3}$ at 26% RH and $1 \times 10^{17} \text{ photons cm}^{-2} \text{ s}^{-1}$ (Stemmler et al., 2007), black circles = gentisic acid
 8 coating ($160\text{-}200 \mu\text{g cm}^{-2}$) at 40-45% RH and light intensity similar as in the humic acid aerosol **ease** study (Sosedova et al.,
 9 2011), green diamonds = ortho-nitrophenol in gas phase (ppm level) illuminated with UV/VIS light. -Dotted lines are
 10 **exponential fittings of the measured data points and are guiding the eyes.**

11

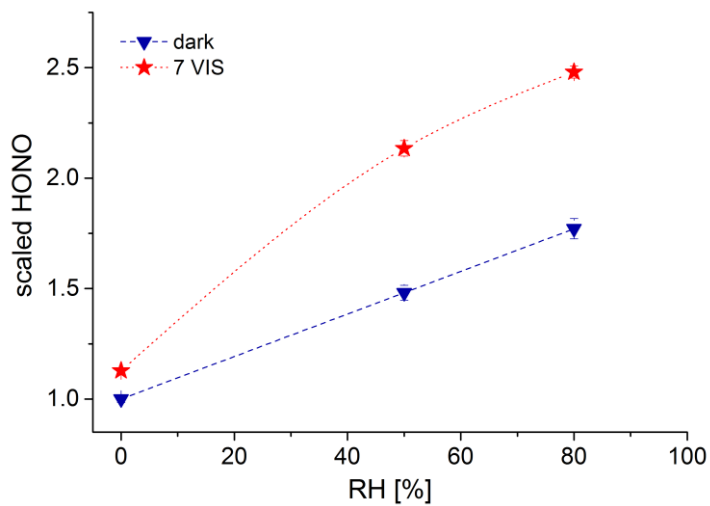
12



3 Fig. 6: HONO formation on three different BSA coating thicknesses, exposed to 20 ppb of NO₂ under illuminated
 4 conditions (7 VIS lamps). The HONO concentrations were **normalizscaled** to reaction tube coverage (black: 100% of
 5 reaction tube was covered with BSA, blueish: 70% of tube was covered and red: 50% of tube was covered with BSA). The
 6 middle thick coating (22.46 µg cm⁻²) was replicated and studied with different reaction times (cyan and blue triangle).
 7 Solid lines (with circles or triangles) present continuous measurements, when those are interrupted other conditions (e.g.
 8 light intensity, NO₂ concentration) prevailed. Dotted lines show interpolations **and are for guiding the eyes**. Arrows
 9 indicate the intervals in which the shown decay rates were determined. Error bars indicates standard deviations from 10-
 10 20 measuring points (5-10 min).

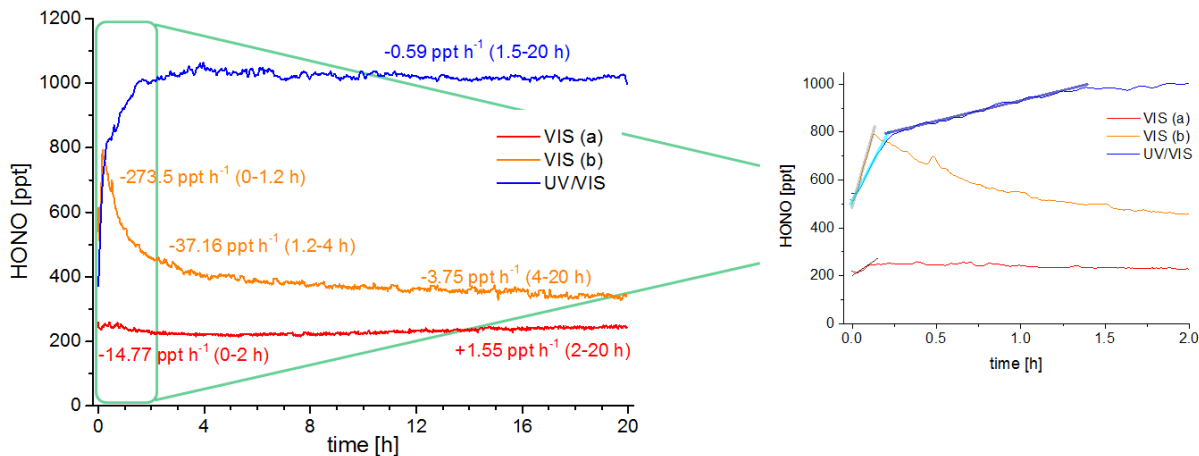


1



2

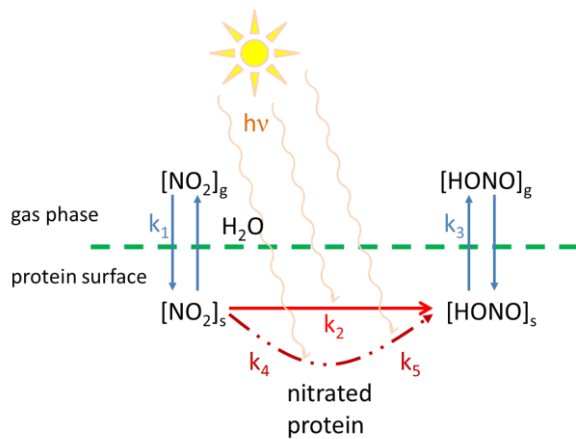
3 **Fig. 7: Dependency of relative humidity on HONO formation.**
 4 **the transformation of 25 ppb NO₂ was applied on BSA**
 5 **surface (17.5 μg cm⁻²) either in darkness (blue triangle) and/or with 7 VIS lights (red star). HONO was normalized/scaled**
 6 **to HONO concentrations in darkness under dry conditions ([HONO]_{lights on-off; RH}/[HONO]_{dark; RH=0}). Dotted lines are for**
guiding the eyes.



7

1 | Fig. 8: Extended (~~20 h~~) measurements (20 h) of light-enhanced HONO formation on BSA (three coatings of $17.5 \mu\text{g cm}^{-2}$)
 2 | at 80% RH, 100 ppb NO_2 . HONO formation under VIS light is shown in red and orange, under UV/Vis light in blue.
 3 | HONO decay rates [ppt h^{-1}] are shown with time periods (in brackets) in which they were calculated, suggesting a stable
 4 | HONO formation after 4 hours. Right: zoom in on the first 2 hours. Straight lines (black, grey, light and dark blue) show
 5 | the regressionslopes of which $d[\text{HONO}]/dt$ were used in the kinetic studies.

6
7



8

9 | Fig. 9: Schematic illustration of the underlying Langmuir-Hinshelwood-mechanism of light induced HONO formation on
 10 | protein surface. Reaction constants for NO_2 uptake, direct NO_2 conversion, protein nitration, HONO formation from
 11 | decomposing nitrated proteins and HONO release are indicated by k_1 , k_2 , k_4 , k_5 , and k_3 , respectively.